Inorg. Chem. **2007**, *46*, 10120–10132

Acetonitrile Hydration and Ethyl Acetate Hydrolysis by Pyrazolate-Bridged Cobalt(II) Dimers Containing Hydrogen-Bond Donors

Paul J. Zinn,[†] Thomas N. Sorrell,[‡] Douglas R. Powell,[†] Victor W. Day,[†] and A. S. Borovik*[,†,§]

Department of Chemistry, University of Kansas, 2010 Malott Hall, 1251 Wescoe Hall Drive, Lawrence, Kansas 66045, and Department of Chemistry, University of North Carolina, Chapel Hill, North Carolina 27599

Received April 10, 2007

The preparation of new Co^{II}–μ-OH–Co^{II} dimers with the binucleating ligands 3,5-bis{bis[(*N*′-R-ureaylato)-*N*-ethyl]-aminomethyl}-1*H*-pyrazolate ([H_4**P^{R}buam**]$^{5-}$, R = ^{t}Bu, ^{i}Pr) is described. The molecular structure of the isopropyl derivative reveals that each Co^{II} center has a trigonal-bipyramidial coordination geometry, with a Co···Co separation of 3.5857(5) Å. Structural and spectroscopic studies show that there are four hydrogen-bond (H-bond) donors near the Co^{II}–μ-OH–Co^{II} moiety; however, they are too far away to be form intramolecular H-bonds with the bridging hydroxo ligand. Treating [$Co^{II}_2H_4$**P^{R}buam**(μ-OH)]$^{2-}$ with acetonitrile led to the formation of bridging acetamidato complexes, [$Co^{II}_2H_4$**P^{R}buam**(μ-1,3-OC(NH)CH_3)]$^{2-}$; in addition, these Co^{II}–μ-OH–Co^{II} dimers hydrolyze ethyl acetate to form Co^{II} complexes with bridging acetato ligands. The Co^{II}–1,3-μ-X′–Co^{II} complexes (X′ = OAc^-, [$OC(NH)CH_3$]$^-$) were prepared independently by reacting [$Co^{II}_2H_3$**P^{R}buam**]$^{2-}$ with acetamide or [$Co^{II}_2H_4$**P^{R}buam**]$^-$ with acetate. X-ray diffraction studies show that the orientation of the acetate ligand within the H-bonding cavity depends on the size of the R substituent appended from the urea groups. The tetradentate ligand 3-{bis[(*N*′-*tert*-butylureaylato)-*N*-ethyl]aminomethyl}-5-*tert*-butyl-1*H*-pyrazolato ([H_2**P$^{t\text{Bu}}$uam**]$^{3-}$) was also developed and its Co^{II}–OH complex prepared. In the crystalline state, [$Co^{II}H_2$**P$^{t\text{Bu}}$uam**(OH)]$^{2-}$ contains two intramolecular H-bonds between the urea groups of [H_2**P$^{t\text{Bu}}$uam**]$^{3-}$ and the terminal hydroxo ligand. [^{n}Pr_4N]$_2$[$Co^{II}H_2$**P$^{t\text{Bu}}$uam**(OH)] does not hydrate acetonitrile or hydrolyze ethyl acetate. In contrast, K_2[$Co^{II}H_2$**P$^{t\text{Bu}}$uam**(OH)] does react with ethyl acetate to produce KOAc; this enhanced reactivity is attributed to the presence of the K^+ ions, which can possibly interact with the Co^{II}–OH unit and ester substrate to assist in hydrolysis. However, K_2[$Co^{II}H_2$**P$^{t\text{Bu}}$uam**(OH)] was still unable to hydrate acetonitrile.

Introduction

The hydration and hydrolysis of unactivated molecules is an area of synthetic interest for the preparation of industrially and pharmacologically important compounds.[1] For instance, the hydration of nitriles can be applied for more efficient synthesis of amides such as acrylamide or nicotinamide. However, the preparation of amides through standard base- or acid-catalyzed reactions has several limitations and/or disadvantages.[2] The difficulties in the preparation of amides through the hydration of nitriles can be overcome through the utilization of metal ions. In spite of numerous reports on the metal-mediated processes,[1] the use of synthetic Co^{II} complexes in investigating these types of reactivities remains relatively unexplored.[3]

In most metal-based systems that perform this chemistry, a metal−hydroxo unit is proposed to be the active species. For example, the active sites of multinuclear metallohydro-

* To whom correspondence should be addressed. E-mail: aborovik@uci.edu.
† University of Kansas.
‡ University of North Carolina.
§ Current address: Department of Chemistry, University of California, Irvine, CA 92697.

(1) Kukushkin, V. Y.; Pombeiro, A. J. L. *Inorg. Chim. Acta* **2005**, *358*, 1−21 and references cited therein.

(2) (a) Parkins, A. W. *Platinum Met. Rev.* **1996**, *40*, 169−174 and references cited therein. (b) Ghaffar, T.; Parkins, A. W. *J. Mol. Catal. A: Chem.* **2000**, *160*, 249−261. (c) Murahashi, S.-I.; Takaya, H. *Acc. Chem. Res.* **2000**, *33*, 225−233.

(3) Only Co^{II} metal salts have been used: (a) Clarke, C. R.; Hay, R. W. *Dalton Trans.* **1974**, 2148−2152. (b) Segl'a, P.; Jamnicky, M.; Koman, M.; Sima, J.; Glowiak, T. *Polyhedron* **1998**, *17*, 4525−4533. (c) Kopylovich, M. N.; Kukushkin, V. Y.; Guedes da Silva, M. F. C.; Haukka, M.; Fraústo da Silva, J. J. R.; Pombeiro, A. J. L. *J. Chem. Soc., Perkin Trans. 1* **2001**, 1569−1573.

10.1021/ic700685g CCC: $37.00 © 2007 American Chemical Society
Published on Web 11/01/2007

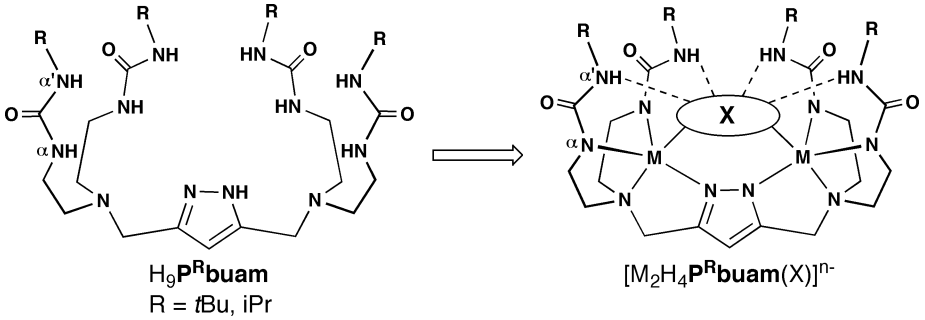

Figure 1. Dinucleating ligand and general dinuclear complex with an exogenous ligand (X) accepting H-bonds donated by the unsymmetrical urea chelates.

lases, metal-containing enzymes that efficiently catalyze the hydrolysis of unactivated substrates such as DNA, peptides, and urea, are proposed to contain two kinds of active metal−hydroxo species: (i) a M(M−OH) species where the hydroxo ligand is coordinated to one metal site of the dinuclear center in a terminal fashion and (ii) a M−μ-OH−M moiety containing a μ-hydroxo ligand bridged between the two metal ions.[4] X-ray diffraction and spectroscopic studies on many of these enzymes suggest that basic functionalities such as carboxylates are used to scavenge protons liberated during the formation of M−OH moieties. In addition, intramolecular hydrogen bonds (H-bonds) between amino acid residues of the protein backbone and external ligands coordinated to the active-site metal ions are found to effectively control metal-mediated hydrolysis while adding structural stability.[5] These studies illustrate the need to control both primary and secondary coordination spheres about the M−OH unit to achieve efficient hydration/hydrolysis of unactivated compounds.

Synthetic systems that contain many of these structural attributes have been prepared, and some structure−function studies have been reported.[6] Notable examples include the works of Berreau and Marques-Rivas, who have shown that intramolecular H-bonds affect the physical and chemical properties of Zn^{II}−OH units.[7−9] We have also developed systems that utilize intramolecular H-bonds to influence metal-ion-mediated processes.[10,11] Recently, we have developed dinucleating ligands (H$_9$**P^{R}buam**; R = ^{t}Bu or ^{i}Pr) that are capable of forming cavities comprised of four H-bond donors upon chelating two metal ions within close proximity (Figure 1).[12,13] Deprotonation of the pyrazole and the urea αNH groups provides a primary coordination sphere for each metal ion comprised of two urea αN$^-$ donors, one pyrazolate N atom, an apical amine N atom, and an exogenous bridging ligand arranged in a distorted trigonal-bipyramidal geometry. The urea arms are sufficiently rigid to position four α'NH groups proximal to the metal centers, enforcing intramolecular H-bonds with external species (X) that bind within the cavity. Further control of the secondary coordination sphere originates in the steric demand exhibited by the different R groups appended to the ends of the unsymmetrical urea arms. These effects were illustrated in the molecular structures of cobalt dimers with Co^{II}−μ-Cl−Co^{II} motifs; the chloro ligands were involved in four additional intramolecular H-bonds.[12] These noncovalent interactions appear to influence the length of the Co^{II}−Cl bonds, which were unusually long at distances greater than 2.6 Å.

We now report the preparation of new cobalt dimers with Co^{II}−μ-OH−Co^{II} moieties. During the course of this study,

(4) (a) Sträter, N.; Lipscomb, W. N.; Klabunde, T.; Krebs, B. *Angew. Chem., Int. Ed. Engl.* **1996**, *35*, 2024−2055. (b) Wilcox, D. E. *Chem. Rev.* **1996**, *96*, 2435−2458.

(5) (a) Vobeda, A.; Lahm, A.; Sakiyama, F.; Suck, D. *EMBO J.* **1991**, *10*, 1607−1618. (b) Chevrier, B.; Schalk, C.; D'Orchymont, H.; Rondeau, J.-M.; Moras, D.; Tarnus, C. *Structure* **1994**, *2*, 283−291. (c) Romier, C.; Dominguez, R.; Lahm, A.; Dahl, O.; Suck, D. *Proteins* **1998**, *32*, 414−424. (d) Desmarais, W. T.; Bienvenue, D. L.; Bzymek, K. P.; Holz, R. C.; Petsko, G. A.; Ringe, D. *Structure* **2002**, *10*, 1063−1072. (e) Bzymek, K. P.; Moulin, A.; Swierczek, S. I.; Ringe, D.; Petsko, G. A.; Bennett, B.; Holz, R. C. *Biochemistry* **2005**, *44*, 12030−12040. (f) Bzymek, K. P.; Swierczek, S. I.; Bennett, B.; Holz, R. C. *Inorg. Chem.* **2005**, *44*, 8574−8580.

(6) For recent examples, see: (a) Wada, A.; Harata, M.; Hasegawa, K.; Jitsukawa, K.; Masuda, H.; Mukai, M.; Kitagawa, T.; Einaga, H. *Angew. Chem., Int. Ed.* **1998**, *37*, 798−799. (b) Matsu-ura, M.; Tani, F.; Nakayama, S.; Nakamura, N.; Naruta, Y. *Angew. Chem., Int. Ed.* **2000**, *39*, 1989−1991. (c) Grotjahn, D. B.; Incarvito, C. D.; Rheingold, A. L. *Angew. Chem., Int. Ed.* **2001**, *40*, 3884−3887. (d) Garner, D. K.; Fitch, S. B.; McAlexander, L. H.; Bezold, L. M.; Arif, A. M.; Berreau, L. M. *J. Am. Chem. Soc.* **2002**, *124*, 9970−9971. (e) Chang, C. J.; Chng, L. L.; Nocera, D. G. *J. Am. Chem. Soc.* **2003**, *125*, 1866−1876. (f) Rivera, G.; Crabtree, R. H. *J. Mol. Catal. A: Chem.* **2004**, *222*, 59−73.

(7) Dinuclear complex: Allred, R. A.; Doyle, K.; Arif, A. M.; Berreau, L. M. *Inorg. Chem.* **2006**, *45*, 4097−4108.

(8) Mononuclear complexes: (a) Kövári, E.; Krämer, R. *J. Am. Chem. Soc.* **1996**, *118*, 12704−12709. (b) Krämer, R. *Coord. Chem. Rev.* **1999**, *182*, 243−261. (c) Wall, M.; Linkletter, B.; Williams, D.; Lebuis, A.-M.; Hynes, R. C.; Chin, J. *J. Am. Chem. Soc.* **1999**, *121*, 4710−4711. (d) Forconi, M.; Williams, N. H. *Angew. Chem., Int. Ed.* **2002**, *41*, 849−852. (e) Ait-Haddou, H.; Sumaoka, J.; Wiskur, S. L.; Folmer-Andersen, J. F.; Anslyn, E. V. *Angew. Chem., Int. Ed.* **2002**, *41*, 4014−4016. (f) Livieri, M.; Mancin, F.; Tonellato, U.; Chin, J. *Chem. Commun.* **2004**, *24*, 2862−2863. (g) Feng, G.; Mareque-Rivas, J. C.; Martin de Rosales, R. T.; Williams, N. H. *J. Am. Chem. Soc.* **2005**, *127*, 13470−13471.

(9) Feng, G.; Mareque-Rivas, J. C.; Williams, N. H. *Chem. Commun.* **2006**, 1845−1847.

(10) (a) Hammes, B. S.; Young, V. G., Jr.; Borovik, A. S. *Angew. Chem., Int. Ed.* **1999**, *38*, 666−669. (b) MacBeth, C. E.; Golombek, A. P.; Young, V. G., Jr.; Yang, C.; Kuczera, K.; Hendrich, M. P.; Borovik, A. S. *Science* **2000**, *289*, 938−941. (c) Larsen, P. L.; Gupta, R.; Powell, D. R.; Borovik, A. S. *J. Am. Chem. Soc.* **2004**, *126*, 6522−6523. (d) MacBeth, C. E.; Gupta, R.; Mitchell-Koch, K. R.; Young, V. G., Jr.; Lushington, G. H.; Thompson, W. H.; Hendrich, M. P.; Borovik, A. S. *J. Am. Chem. Soc.* **2004**, *126*, 2556−2567. (e) Borovik, A. S. *Acc. Chem. Res.* **2005**, *38*, 54−61. (f) Lucas, R. L.; Powell, D. R.; Borovik, A. S. *J. Am. Chem. Soc.* **2005**, *127*, 11596−11597.

(11) MacBeth, C. E.; Hammes, B. S.; Young, V. G., Jr.; Borovik, A. S. *Inorg. Chem.* **2001**, *40*, 4733−4741.

(12) Zinn, P. J.; Powell, D. R.; Day, V. W.; Hendrich, M. P.; Sorrell, T. N.; Borovik, A. S. *Inorg. Chem.* **2006**, *45*, 3484−3486.

(13) Another dinucleating ligand containing H-bond donors has been reported: Arii, H.; Funahashi, Y.; Jitsukawa, K.; Masuda, H. *Dalton Trans.* **2003**, 2115−2116.

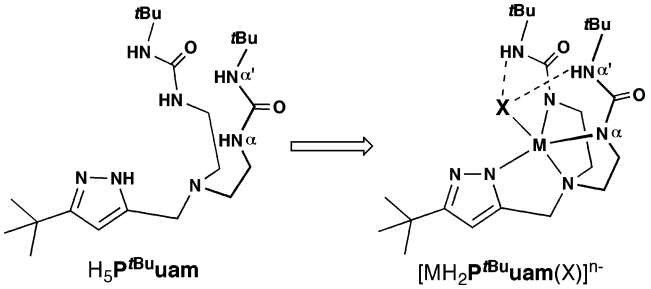

Figure 2. Mononucleating ligand, $H_5\mathbf{P^{tBu}uam}$, and general mononuclear complex with an additional ligand (X).

we have found that these complexes can hydrate unactivated nitriles and hydrolyze unactivated esters, such as acetonitrile and ethyl acetate, at room temperature. Isolation and structural characterization of the hydration/hydrolysis products confirm that bridging acetamidate or acetate ligands are present. In a comparative study, we have developed a related monomeric Co^{II} complex with a terminal hydroxo ligand (Figure 2) and investigated its hydrolytic properties. The results of these studies have provided insights into the role that the metal centers and H-bond networks have on the observed reactivity.

Experimental Section

General Methods. All reagents were purchased from commercial sources and used as received, unless otherwise noted. Solvents were purified according to standard procedures.[14] Anhydrous solvents were purchased from Aldrich. Anhydrous *N*,*N*-dimethylacetamide (DMA), CH_2Cl_2, and CH_3CN were eluted through a column of alternating bands of silica gel and neutral alumina and stored over molecular sieves before use. Potassium hydride (KH) as a 30% dispersion in mineral oil was filtered with a medium-porosity glass frit and washed five times each with pentane and Et_2O. The solid KH was dried under vacuum and stored under an inert atmosphere. The syntheses of metal complexes were conducted in a Vacuum Atmospheres Co. drybox under an argon atmosphere. Elemental analyses were accomplished at Desert Analytics (Tucson, AZ). The binucleating ligands 3,5-bis{bis[(*N*′-R-ureayl)-*N*-ethyl]aminomethyl}-1*H*-pyrazole ($H_9\mathbf{P^R uam}$, R = ^{t}Bu, ^{i}Pr),[12] 6-[(tetrahydro-2*H*-pyran-2-yl)oxy]-2,2-dimethylpent-4-yn-3-one,[15] and bis[(*N*′-*tert*-butylureayl)-*N*-ethyl]amine ($^{t\mathbf{Bu}}\mathbf{N_5}$)[16] were prepared by literature methods.

Ligand Synthesis. 3-(Chloromethyl)-5-*tert*-butyl-1-(tetrahydropyran-2-yl)-1*H*-pyrazole (1). Following a modified procedure based on a synthetic route reported by Grotjahn et al.,[15] crude 6-[(tetrahydro-2*H*-pyran-2-yl)oxy]-2,2-dimethylpent-4-yn-3-one (7.29 g, 32.5 mmol) was dissolved in MeOH (33 mL) in a 100 mL round-bottomed flask. Hydrazine monohydrate (1.64 g, 32.8 mmol) was added very slowly to the solution (exothermic reaction). The reaction mixture became hot and started to reflux. The resulting room temperature mixture was allowed to stir for 3 h. Concentrated HCl was then added until the solution reached pH 2, and it was subsequently stirred for 19 h. The solvent was removed under reduced pressure in the same flask to obtain a dark-orange, oily solid. The oily solid was placed under vacuum for 2 h to remove as many volatile components as possible. Next, thionyl chloride (24.7 g, 208 mmol) was introduced to the dark-orange residue and stirred for 17 h. $SOCl_2$ was removed under reduced pressure to produce a brown, sticky solid. Following a similar procedure developed by Meyer,[17] the resulting crude 5-*tert*-butyl-3-(chloromethyl)pyrazole hydrochloride was dissolved in CH_2Cl_2 and 1,2-dihydropyran (6.12 g, 72.8 mmol) was added. The dark-brown solution was stirred for 27 h. The mixture was then washed with a solution of 16.6 g of sodium bicarbonate in 270 mL of water, and the organic phase was dried over magnesium sulfate. The organic phase was filtered, and the filtrate was concentrated under reduced pressure to afford a dark-brown oil, which was eluted through a column of silica gel using 10% Et_2O/hexanes. The product was isolated (R_f = 0.25; 10% Et_2O/hexanes and silica gel) as a light-orange oil, which was then dissolved in a minimal amount of hexanes and placed in a freezer overnight, resulting in an off-white, microcrystalline solid. This microcrystalline solid was filtered, washed with cold hexanes, and placed under vacuum to dry. Recrystallization was repeated with the filtrate several times to obtain a total of 4.77 g (57%). Mp: 39−41 °C. HRMS (ESI, *m/z*): 257.1427 [M^+]. Exact mass calcd for $C_{13}H_{22}N_2O_1Cl_1$ [M + H]: 257.1421. ^{1}H NMR ($CDCl_3$): δ 6.18 (s, 1H, Pz−*H*^{4}), 5.43 (dd, *J* = 2.7 and 9.5 Hz, 1H, *H*^{2}−thp), 4.71 (pseudo-d, *J* = 12.6 Hz, 1H, Pz−C^3−C*H*$_2$), 4.65 (pseudo-d, *J* = 12.6 Hz, 1H, Pz−C^3−C*H*$_2$), 4.01 (m, 1H, *H*^{6}−thp), 3.68 (m, 1H, *H*^{6}−thp), 2.43 (m, 1H, *H*^{3}−thp), 2.10 (m, 1H, *H*^{3}−thp), 2.00 (m, 1H, *H*^{4}−thp), 1.73−1.57 (m, 3H, *H*^{4}/*H*^{5}−thp), 1.28 (s, 9H, (C(C*H*$_3$)). ^{13}C NMR ($CDCl_3$): δ 160.94 (Pz−*C*^{5}), 138.23 (Pz−*C*^{3}), 104.86 (Pz−*C*^{4}), 85.55 (*C*^{2}−thp), 67.72 (*C*^{6}−thp), 35.28 (Pz−C^3−*C*H$_2$Cl), 32.27 (*C*(CH$_3$)), 30.54 (C(*C*H$_3$)$_3$), 29.52 (*C*^{3}−thp), 25.13 (*C*^{5}−thp), 22.66 (*C*^{4}−thp).

3-{Bis[(*N*′-*tert*-butylureayl)-*N*-ethyl]aminomethyl}-5-*tert*-butyl-1-(tetrahydropyran-2-yl)-1*H*-pyrazole (2). A mixture of **1** (3.77 g, 14.7 mmol), $^{t\mathbf{Bu}}\mathbf{N_5}$ (4.64 g, 15.4 mmol), oven-dried sodium carbonate (7.79 g, 73.5 mmol), and anhydrous acetonitrile (150 mL) was refluxed under nitrogen for 24 h. Thin-layer chromatography (TLC) indicated that **1** was not present in the reaction mixture (R_f = 0.34; silica gel TLC and 10% Et_2O/hexanes) after 24 h. The boiling reaction mixture was filtered, and the white solid was washed with boiling acetonitrile. The solvent was then removed from the combined filtrate under reduced pressure, resulting in a yellow-orange solid. Next, the solid was dissolved in boiling acetone, concentrated to saturation, and allowed to cool to room temperature. The solution was placed in a freezer (∼−20 °C) overnight to produce an off-white, microcrystalline solid. The recrystallized product was filtered, washed with cold diethyl ether, and dried under vacuum. Additional product was obtained by repeating the recrystallization with the filtrate, affording a total of 6.49 g (85%). Mp: 106−108 °C. LRMS (FAB$^+$; *m/z*): 522.5 [M^+]. IR (KBr, cm^{-1}): ν(NH) 3377, ν(NH) 3291, ν(CO) 1645, ν(NH) 1563. ^{1}H NMR ($CDCl_3$): δ 6.00 (s, 1H, Pz−*H*^{4}), 5.37 (dd, *J* = 2.6 and 9.7, 1H, *H*^{2}−thp), 5.04 (t, *J* = 4.9 Hz, 2H, CH$_2$N*H*−C(O)), 4.71 (s, 2H, N*H*−C(CH$_3$)$_3$), 4.05 (m, 1H, H^6−thp), 3.66 (m, 1H, H^6−thp), 3.62 (pseudo-d, *J* = 13.9 Hz, 1H, Pz−C^3−C*H*$_2$), 3.54 (pseudo-d, *J* = 13.9 Hz, 1H, Pz−C^3−C*H*$_2$), 3.29 (m, 2H, CH$_2$C*H*$_2$-NH), 3.09 (m, 2H, CH$_2$C*H*$_2$NH), 2.53 (t, *J* = 4.9 Hz, 4H, NC*H*$_2$-CH$_2$), 2.51 (m, 1H, *H*^{3}−thp), 2.08 (m, 1H, *H*^{4}−thp), 1.86 (m, 1H, *H*^{3}−thp), 1.69−1.56 (m, 3H, *H*^{4}/*H*^{5}−thp), 1.32 (s, 18H, NH−C(C*H*$_3$)$_3$), 1.27 (s, 9H, Pz−C^5−C(C*H*$_3$)$_3$). ^{13}C NMR ($CDCl_3$): δ 160.91 (Pz−*C*^{5}), 158.25 (*C*(O)), 140.21 (Pz−*C*^{3}), 104.85 (Pz−*C*^{4}), 84.23 (*C*^{2}−thp), 67.56 (*C*^{6}−thp), 54.81 (NCH$_2$CH$_2$), 50.30

(14) Perrin, D. D.; Armarego, W. L. F. *Purification of Laboratory Chemicals*, 3rd ed.; Pergamon Press: Elmsford, NY, 1988.
(15) Grotjahn, D. B.; Van, S.; Combs, D.; Lev, D. A.; Schneider, C.; Rideout, M.; Meyer, C.; Hernandez, G.; Mejorado, L. *J. Org. Chem.* **2002**, *67*, 9200−9209.
(16) Lucas, R. L. Ph.D. Dissertation, University of Kansas, Lawrence, KS, 2005.
(17) Röder, J. C.; Meyer, F.; Pritzkow, H. *Organometallics* **2001**, *20*, 811−817.

(Pz−C^3−CH_2N), 49.95 (NH−C(CH_3)$_3$), 38.19 (CH_2CH_2NH), 32.28 (Pz−C^5−C(CH_3)$_3$), 30.67 (Pz−C^5−C(CH_3)$_3$), 29.76 (NH−C(CH_3)$_3$), 29.65 (C^3−thp), 25.17 (C^5−thp), 22.81 (C^4−thp).

3-{Bis[(*N*′-*tert*-butylureayl)-*N*-ethyl]aminomethyl}-5-*tert*-butyl-1*H*-pyrazole (H_5P^{tBu}uam). To a solution of **2** (6.49 g, 12.4 mmol) in absolute ethanol (118 mL) was added 67 mL of freshly prepared ethanolic HCl, and the reaction mixture was stirred at room temperature for 18 h. The solvent was removed under reduced pressure to obtain an off-white solid. Next, the solid was dissolved in water (100 mL), and 100 mL of a saturated sodium carbonate solution was added, resulting in a white precipitate. The pH of the aqueous solution was ≥8. The precipitated product was then extracted with three 200 mL portions of dichloromethane, and the combined organic layer was dried with sodium sulfate. The mixture was filtered, and the filtrate was concentrated under reduced pressure to yield an off-white solid, 5.34 g (98%). X-ray-quality crystals were obtained by slow evaporation of a $CHCl_3$ solution of the product. Mp: 115−117 °C. HRMS (ESI, *m/z*): 438.3564 [M^+]. Exact mass calcd for $C_{22}H_{44}N_7O_2$ [M + H]: 438.3556. IR (KBr, cm^{-1}): ν(NH) 3369, ν(NH) 3296, ν(NH) 3214, ν(CO) 1640, ν(NH) 1561. ^{1}H NMR ($CDCl_3$): δ 5.95 (s, 1H, Pz−H^4), 5.72 (bs, 2H, CH_2NH−C(O)), 5.16 (s, 2H, NH−C(CH_3)$_3$), 3.61 (s, 2H, Pz−C^3−CH_2), 3.17 (bs, 4H, CH_2CH_2NH), 2.52 (t, J = 5.0 Hz, 4H, NCH_2CH_2), 1.33 (s, 18H, NH−C(CH_3)$_3$), 1.30 (s, 9H, Pz−C^5−C(CH_3)$_3$). ^{13}C NMR ($CDCl_3$): δ 159.18 (C(O)), 101.60 (Pz−C^4), 55.06 (NCH_2CH_2), 51.11 (NH−C(CH_3)$_3$), 50.46 (Pz−C^3−CH_2N), 38.17 (CH_2CH_2NH), 31.94 (Pz−C^5−C(CH_3)$_3$), 30.88 (Pz−C^5−C(CH_3)$_3$), 30.01 (NH−C(CH_3)$_3$). Note: Quaternary carbons Pz−C^3 and Pz−C^5 are not observed by ^{13}C NMR.

Complex Synthesis. Tetrapropylammonium or Tetraethylammonium μ-Hydroxo-μ-{3,5-bis{bis[(*N*′-*tert*-butylureaylato)-*N*-ethyl]aminatomethyl}-1*H*-pyrazolato}dicobaltate(II) ($[^nPr_4N]_2$-$[Co^{II}_2H_4P^{tBu}$buam(μ-OH)]) or ($[Et_4N]_2[Co^{II}_2H_4P^{tBu}$buam($\mu$-OH)]). A solution of 3,5-bis{bis[(*N*′-*tert*-butylureayl)-*N*-ethyl]aminomethyl}-1*H*-pyrazole (H_9P^{tBu}**buam**; 0.100 g, 0.144 mmol) in anhydrous DMA (5 mL) was treated with solid KH (0.035 g, 0.86 mmol) under an argon atmosphere. After gas evolution ceased, solid $CoCl_2$ (0.037 g, 0.29 mmol) was added. The resulting turquoise-blue solution was stirred for 30 min. Ultrapure H_2O (0.0026 g, 0.14 mmol) was added by microsyringe, resulting in a purple solution, with stirring continued for an additional 30 min. Tetrapropylammonium chloride (0.064 g, 0.29 mmol) or tetraethylammonium chloride (0.048 g, 0.29 mmol) was then added and stirred for 1 h. The solvent was removed under reduced pressure at room temperature, and the resulting solid residue was washed with diethyl ether and dried under vacuum to afford a purple powder. The powder was then dissolved in anhydrous CH_2Cl_2, and the insoluble KCl was filtered using a fine-porosity glass frit. The solvent was evaporated from the filtrate under reduced pressure to afford a purple solid, 0.18 g (99+%). X-ray-quality crystals were obtained by vapor diffusion of diethyl ether in a DMA solution of the isolated metal salt. Anal. Calcd (found) for $[Et_4N]_2[Co^{II}_2H_4P^{tBu}$**buam**($\mu$-OH)]·0.5$CH_2Cl_2$, $C_{49.5}H_{103}ClCo_2N_{14}O_5$: C, 52.72 (53.03); H, 9.21 (8.73); N, 17.39 (17.40). Anal. Calcd (found) for $[^nPr_4N]_2$-$[Co^{II}_2H_4P^{tBu}$**buam**(μ-OH)], $C_{57}H_{118}Co_2N_{14}O_5$: C, 57.17 (57.26); H, 9.93 (9.76); N, 16.38 (15.90). IR (Nujol, cm^{-1}): ν(OH) 3620, ν(NH) 3352, 3294, ν(CO) 1637, 1587. UV/vis (DMA): λ_{max}, nm (ϵ, M^{-1} cm^{-1}) 503 (sh), 562 (260), 930 (36).

Tetrapropylammonium μ-Hydroxo-μ-{3,5-bis{bis[(*N*′-isopropylureaylato)-*N*-ethyl]aminatomethyl}-1*H*-pyrazolato}dicobaltate(II) ($[^nPr_4N]_2[Co^{II}_2H_4P^{iPr}$buam($\mu$-OH)]). This compound was prepared by the same route as $[^nPr_4N]_2[Co^{II}_2H_4P^{tBu}$**buam**($\mu$-OH)] using 3,5-bis{bis[(*N*′-isopropylureayl)-*N*-ethyl]aminomethyl}-1*H*-pyrazole (H_9P^{iPr}**buam**; 0.100 g, 0.157 mmol), KH (0.038 g, 0.94 mmol), $CoCl_2$ (0.041 g, 0.31 mmol), H_2O (0.0028 g, 0.16 mmol), and tetrapropylammonium chloride (0.070 g, 0.31 mmol) to yield a purple solid, 0.17 g (94%). X-ray-quality crystals were obtained by vapor diffusion of diethyl ether in a DMA solution of the isolated metal salt. Anal. Calcd (found) for $[^nPr_4N]_2[Co^{II}_2H_4P^{iPr}$**buam**($\mu$-OH)]·0.1$CH_2Cl_2$, $C_{53.1}H_{110.2}Cl_{0.2}Co_2N_{14}O_5$: C, 55.46 (55.98); H, 9.66 (9.24); N, 17.05 (16.60). IR (Nujol, cm^{-1}): ν(OH) 3612, ν(NH) 3348, ν(CO) 1637, 1582. UV/vis (DMA): λ_{max}, nm (ϵ, M^{-1} cm^{-1}) 508 (sh), 560 (250), 847 (37).

Tetrapropylammonium or Tetraethylammonium μ-1,3-Acetamidato-μ-{3,5-bis{bis[(*N*′-*tert*-butylureaylato)-*N*-ethyl]aminatomethyl}-1*H*-pyrazolato}dicobaltate(II) ($[^nPr_4N]_2[Co^{II}_2H_4P^{tBu}$buam($\mu$-1,3-OC(NH)$CH_3$)]) or ($[Et_4N]_2[Co^{II}_2H_4P^{tBu}$buam($\mu$-1,3-OC(NH)$CH_3$)]). A solution of H_9P^{tBu}**buam** (0.100 g, 0.144 mmol) in anhydrous DMA (5 mL) was treated with solid KH (0.035 g, 0.86 mmol) under an argon atmosphere. After gas evolution ceased, solid $CoCl_2$ (0.037 g, 0.29 mmol) was added. The resulting turquoise-blue solution was stirred for 30 min. Next, acetamide (0.009 g, 0.14 mmol) was added, resulting in a violet solution while being stirred for an additional 30 min. Tetrapropylammonium chloride (0.064 g, 0.29 mmol) or tetraethylammonium chloride (0.048 g, 0.29 mmol) was then added and stirred for 1 h. The solvent was removed under reduced pressure at room temperature, and the resulting solid residue was washed with diethyl ether and dried under vacuum to afford a violet powder. The powder was then dissolved in anhydrous CH_2Cl_2, and the insoluble KCl was filtered using a fine-porosity glass frit. The solvent was evaporated from the filtrate under reduced pressure to afford a violet solid, 0.19 g. X-ray-quality crystals were obtained by vapor diffusion of diethyl ether in a DMA solution of the isolated metal salt. Anal. Calcd (found) for $[Et_4N]_2[Co^{II}_2H_4P^{tBu}$**buam**($\mu$-1,3-OC(NH)$CH_3$)], $C_{51}H_{105}Co_2N_{15}O_5$: C, 54.38 (54.57); H, 9.40 (9.22); N, 18.65 (18.34). $[^nPr_4N]_2[Co^{II}_2H_4P^{tBu}$**buam**($\mu$-1,3-OC(NH)$CH_3$)]. IR (Nujol, cm^{-1}): ν(NH) 3406, 3304, ν(CO) 1639, 1583, ν(NCO) 1539, 1516. UV/vis (DMA): λ_{max}, nm (ϵ, M^{-1} cm^{-1}) 484 (sh), 542 (240), 718 (40).

Tetrapropylammonium μ-1,3-Acetamidato-μ-{3,5-bis{bis[(*N*′-isopropylureaylato)-*N*-ethyl]aminatomethyl}-1*H*-pyrazolato}-dicobaltate(II) ($[^nPr_4N]_2[Co^{II}_2H_4P^{iPr}$buam($\mu$-1,3-OC(NH)$CH_3$)]). This compound was prepared by the same route as $[^nPr_4N]_2$-$[Co^{II}_2H_4P^{tBu}$**buam**(μ-1,3-OC(NH)CH_3)] using H_9P^{iPr}**buam** (0.100 g, 0.157 mmol), KH (0.038 g, 0.94 mmol), $CoCl_2$ (0.041 g, 0.31 mmol), acetamide (0.009 g, 0.16 mmol), and tetrapropylammonium chloride (0.070 g, 0.31 mmol) to yield a violet solid, 0.19 g (99+%). X-ray-quality crystals were obtained by vapor diffusion of diethyl ether in a DMA solution of the isolated metal salt. Anal. Calcd (found) for $[^nPr_4N]_2[Co^{II}_2H_4P^{iPr}$**buam**($\mu$-1,3-OC(NH)$CH_3$)], $C_{55}H_{113}Co_2N_{15}O_5$: C, 55.87 (56.40); H, 9.63 (9.38); N, 17.77 (17.46). IR (Nujol, cm^{-1}): ν(NH) 3415, 3289, ν(CO) 1577, ν(NCO) 1538, 1494. UV/vis (DMA): λ_{max}, nm (ϵ, M^{-1} cm^{-1}) 480 (sh), 542 (220), 720 (34).

Tetrapropylammonium μ-1,3-Acetato-μ-{3,5-bis{bis[(*N*′-*tert*-butylureaylato)-*N*-ethyl]aminatomethyl}-1*H*-pyrazolato}dicobaltate(II) ($[^nPr_4N]_2[Co^{II}_2H_4P^{tBu}$buam($\mu$-1,3-OAc)]). A solution of H_9P^{tBu}**buam** (0.100 g, 0.144 mmol) in anhydrous DMA (5 mL) was treated with solid KH (0.029 g, 0.72 mmol) under an argon atmosphere. After gas evolution ceased, solid $Co(OAc)_2$ (0.051 g, 0.29 mmol) was added. The resulting violet solution was stirred for 30 min. Tetrapropylammonium chloride (0.064 g, 0.29 mmol) was then added and stirred for 1 h. The solvent was removed under reduced pressure at room temperature, and the resulting solid residue was washed with diethyl ether and dried under vacuum to afford a

purple powder. The powder was then dissolved in anhydrous CH_2Cl_2, and the insoluble KCl and KOAc were filtered using a fine-porosity glass frit. The solvent was evaporated from the filtrate under reduced pressure to afford 0.18 g of a violet solid. X-ray-quality crystals were obtained by vapor diffusion of diethyl ether in a DMA solution of the isolated metal salt. Anal. Calcd (found) for $[^nPr_4N]_2[Co^{II}_2H_4\mathbf{P^{tBu}buam}(\mu\text{-}1,3\text{-}OAc)]\cdot$DMA, $C_{63}H_{129}Co_2N_{15}O_7$: C, 57.04 (57.24); H, 9.80 (9.53); N, 15.84 (15.49). IR (Nujol, cm^{-1}): ν(NH) 3344, ν(CO) 1580, 1553, 1407. UV/vis (DMA): λ_{max}, nm (ϵ, M^{-1} cm^{-1}) 485 (sh), 502 (sh), 542 (170), 734 (31).

Tetrapropylammonium μ-1,3-Acetato-μ-{3,5-bis{bis[(*N*′-isopropylureaylato)-*N*-ethyl]aminatomethyl}-1*H*-pyrazolato}-dicobaltate(II) ($[^nPr_4N]_2[Co^{II}_2H_4\mathbf{P^{iPr}buam}(\mu\text{-}1,3\text{-}OAc)]$). This compound was prepared by the same route as $[^nPr_4N]_2$ $[Co^{II}_2H_4\mathbf{P^{tBu}buam}(\mu\text{-}1,3\text{-}OAc)]$ using $H_9\mathbf{P^{iPr}buam}$ (0.100 g, 0.157 mmol), KH (0.031 g, 0.79 mmol), $Co(OAc)_2$ (0.056 g, 0.31 mmol), and tetrapropylammonium chloride (0.070 g, 0.31 mmol) to yield 0.19 g of a violet solid. X-ray-quality crystals were obtained by vapor diffusion of diethyl ether in a DMA solution of the isolated metal salt. Anal. Calcd (found) for $[^nPr_4N]_2$ $[Co^{II}_2H_4\mathbf{P^{iPr}buam}(\mu\text{-}1,3\text{-}OAc)]\cdot$DMA, $C_{59}H_{121}Co_2N_{15}O_7$: C, 55.77 (55.10); H, 9.60 (9.74); N, 16.54 (16.26). IR (Nujol, cm^{-1}): ν(NH) 3344, ν(CO) 1640, 1574, 1561, 1411. UV/vis (DMA): λ_{max}, nm (ϵ, M^{-1} cm^{-1}) 484 (sh), 544 (180), 746 (29).

Potassium 3-{Bis[(*N*′-*tert*-butylureaylato)-*N*-ethyl]aminatomethyl}-5-*tert*-butyl-1*H*-pyrazolato(hydroxo)cobaltate(II) ($K_2[Co^{II}H_2\mathbf{P^{tBu}uam}(OH)]$). A solution of $H_5\mathbf{P^{tBu}uam}$ (0.200 g, 0.457 mmol) in anhydrous DMA (5 mL) was treated with solid KH (0.073 g, 1.8 mmol) under an argon atmosphere. After gas evolution ceased, solid $Co(OAc)_2$ (0.081 g, 0.46 mmol) was added. The resulting purple solution was stirred for 30 min and then filtered to separate the precipitated KOAc (0.088 g, 98%) from the reaction mixture. Next, ultrapure H_2O (0.0082 g, 0.46 mmol) was added to the filtrate by microsyringe, resulting in a violet solution, which was stirred for an additional 30 min. The solvent was removed under reduced pressure at room temperature, and the resulting solid residue was washed with diethyl ether, removing a purple, diethyl ether soluble impurity. The solid was subsequently dried under vacuum to afford a violet powder. X-ray-quality crystals were obtained by vapor diffusion of diethyl ether in a DMA solution of the isolated metal salt, 0.29 g (83%). Anal. Calcd (found) for $K_2[Co^{II}H_2\mathbf{P^{tBu}uam}(OH)]\cdot$2DMA, $C_{30}H_{59}CoK_2N_9O_5$: C, 47.23 (47.04); H, 7.79 (7.72); N, 16.52 (16.24). IR (Nujol, cm^{-1}): ν(OH) 3620, ν(NH) 3230, 3140, ν(CO) 1645, 1595. EPR (X-band, DMA, 4 K): $g = 5.13, 4.54, 3.42, 2.75, 1.97$. UV/vis (DMA): λ_{max}, nm (ϵ, M^{-1} cm^{-1}) 465 (sh), 486 (sh), 522 (150), 751 (35). $\mu_{eff} = 4.76\ \mu_B$ (solid, 294 K, $\chi_M^{diam} = -420.85 \times 10^{-6}$).

Tetrapropylammonium 3-{Bis[(*N*′-*tert*-butylureaylato)-*N*-ethyl]aminatomethyl}-5-*tert*-butyl-1*H*-pyrazolato(hydroxo)cobaltate(II) ($[^nPr_4N]_2[Co^{II}H_2\mathbf{P^{tBu}uam}(OH)]$). This compound was prepared by the same route as $K_2[Co^{II}H_2\mathbf{P^{tBu}uam}(OH)]$ with the following exceptions. After the addition of H_2O and stirring for 30 min, tetrapropylammonium chloride (0.203 g, 0.914 mmol) was added and subsequently stirred for 1 h. The isolated purple powder was then dissolved in anhydrous CH_2Cl_2, and the insoluble KCl was filtered using a fine-porosity glass frit. The solvent was evaporated from the filtrate under reduced pressure to afford a sticky purple solid. This solid was washed with 1:1 Et_2O/pentane and dried under vacuum to afford a purple powder, 0.41 g (95%). Anal. Calcd (found) for $[^nPr_4N]_2[Co^{II}H_2\mathbf{P^{tBu}uam}(OH)]\cdot 0.8CH_2Cl_2$, $C_{46.8}H_{98.6}Cl_{1.6}CoN_9O_3$: C, 59.09 (58.80); H, 10.45 (11.13); N, 13.25 (12.95). IR (Nujol, cm^{-1}): ν(OH) 3620, ν(NH) 3268, 3175, ν(CO) 1642, 1587. EPR (X-band, DMA, 77 K): $g = 4.51$. UV/vis (DMA): λ_{max}, nm (ϵ, M^{-1} cm^{-1}) 459 (sh), 537 (sh), 563 (93), 612 (sh), 751 (13).

Hydrolysis Reactions. $[^nPr_4N]_2[Co^{II}_2H_4\mathbf{P^{tBu}buam}(\mu\text{-}OH)]$, $[Et_4N]_2[Co^{II}_2H_4\mathbf{P^{tBu}buam}(\mu\text{-}OH)]$, or $[^nPr_4N]_2[Co^{II}_2H_4\mathbf{P^{iPr}buam}(\mu\text{-}OH)]$ with CH_3CN. The appropriate isolated μ-hydroxo complex was dissolved in anhydrous acetonitrile and stirred for 2 h at room temperature under an argon atmosphere. The solvent was then removed under reduced pressure, and the resulting solid residue was washed with diethyl ether and dried under vacuum to obtain a violet powder. Fourier transform IR (FTIR) and UV/vis spectroscopies confirmed the hydrolysis of acetonitrile by displaying the same features as those observed for the corresponding μ-1,3-acetamidato complex synthesized by the direct route. Alternatively, X-ray-quality crystals of the hydrolysis product were obtained by vapor diffusion of diethyl ether in an acetonitrile solution of the appropriate isolated μ-hydroxo complex. For instance, $[^nPr_4N]_2$-$[Co^{II}_2H_4\mathbf{P^{tBu}buam}(\mu\text{-}OH)]$ (0.050 g, 0.042 mmol) was dissolved in 3−4 mL of anhydrous acetonitrile and crystallized by the diffusion of diethyl ether to afford crystals of $[^nPr_4N]_2[Co^{II}_2H_4\mathbf{P^{tBu}buam}(\mu\text{-}1,3\text{-}OC(NH)CH_3)]$, 0.031 g (60%). $[^nPr_4N]_2[Co^{II}_2H_4\mathbf{P^{iPr}buam}(\mu\text{-}OH)]$ (0.050 g, 0.044 mmol) was used to produce crystals of $[^nPr_4N]_2[Co^{II}_2H_4\mathbf{P^{iPr}buam}(\mu\text{-}1,3\text{-}OC(NH)CH_3)]$ (0.040 g, 77%).

$[^nPr_4N]_2[Co^{II}_2H_4\mathbf{P^{tBu}buam}(\mu\text{-}OH)]$ or $[^nPr_4N]_2[Co^{II}_2H_4\mathbf{P^{iPr}buam}(\mu\text{-}OH)]$ with EtOAc. The appropriate isolated μ-hydroxo complex was dissolved in a 1:1 mixture of anhydrous ethyl acetate and anhydrous DMA and stirred for 2 h at room temperature under an argon atmosphere. The solvent was then removed under reduced pressure, and the resulting solid residue was washed with diethyl ether and dried under vacuum to obtain a violet powder. FTIR and UV/vis spectroscopies confirmed the hydrolysis of ethyl acetate by displaying the same features as those observed for the corresponding μ-1,3-OAc complex synthesized by the direct route. Alternatively, X-ray-quality crystals of the hydrolysis product were obtained by vapor diffusion of diethyl ether in a 1:1 ethyl acetate/DMA solution of the appropriate isolated μ-hydroxo complex. For instance, $[^nPr_4N]_2[Co^{II}_2H_4\mathbf{P^{tBu}buam}(\mu\text{-}OH)]$ (0.050 g, 0.042 mmol) was dissolved in 3−4 mL of 1:1 ethyl acetate/DMA and crystallized by the diffusion of diethyl ether to afford crystals of $[^nPr_4N]_2$-$[Co^{II}_2H_4\mathbf{P^{tBu}buam}(\mu\text{-}1,3\text{-}OAc)]\cdot$DMA, 0.038 g (68%). $[^nPr_4N]_2$-$[Co^{II}_2H_4\mathbf{P^{iPr}buam}(\mu\text{-}OH)]$ (0.050 g, 0.044 mmol) was used to produce crystals of $[^nPr_4N]_2[Co^{II}_2H_4\mathbf{P^{iPr}buam}(\mu\text{-}1,3\text{-}OAc)]\cdot$DMA (0.044 g, 79%).

$K_2[Co^{II}H_2\mathbf{P^{tBu}uam}(OH)]$ with EtOAc. A crystalline compound of $K_2[Co^{II}H_2\mathbf{P^{tBu}uam}(OH)]\cdot$DMA (0.073 g, 0.096 mmol) was dissolved in 2 mL of anhydrous DMA under an argon atmosphere, and 2 mL of anhydrous EtOAc was added. The solution was then set up for crystallization using diethyl ether vapor diffusion. A white, microcrystalline solid immediately appeared. After 48 h, the purple mother liquor was filtered, and the white solid was washed with DMA and then with diethyl ether and dried under vacuum. This yielded 0.009 g of KOAc (100%), which was verified by FTIR (Nujol). The solvent was also removed from the mother liquor. The resulting residue was washed with diethyl ether and dried under vacuum to yield a purple powder. FTIR and UV/vis verified that this purple product was not the hydroxo starting complex.

Physical Methods. NMR spectra were recorded on a Bruker Avance 400 or 500 MHz spectrometer equipped with a Silicon Graphics workstation. Chemical shifts are reported in ppm relative to the residual solvent. Most assignments are based on a series of two-dimensional experiments. Fast atom bombardment mass spectra (FAB-MS) were recorded on a Hewlett-Packard 5989A spectrom-

Table 1. Crystallographic Data for $[^nPr_4N]_2[Co^{II}_2H_4\mathbf{P^{iPr}buam}(\mu\text{-OH})_{0.82}(\mu\text{-Cl})_{0.18}]$,[a] $[^nPr_4N]_2[Co^{II}_2H_4\mathbf{P^{iPr}buam}(\mu\text{-1,3-OC(NH)CH}_3)_{0.90}(Cl)_{0.10}]\cdot$DMA,[b] $[^nPr_4N]_2[Co^{II}_2H_4\mathbf{P^{tBu}buam}(\mu\text{-1,3-OC(NH)CH}_3)]\cdot$DMA, $[^nPr_4N]_2[Co^{II}_2H_4\mathbf{P^{iPr}buam}(\mu\text{-1,3-OAc})]\cdot$DMA, $[^nPr_4N]_2[Co^{II}_2H_4\mathbf{P^{tBu}buam}(\mu\text{-1,3-OAc})]\cdot$DMA, and $K_2[Co^{II}H_2\mathbf{P^{tBu}uam}(OH)]\cdot$2DMA

	salt					
	$[^nPr_4N]_2[Co^{II}_2H_4\mathbf{P^{iPr}buam}(\mu\text{-OH})_{0.82}(\mu\text{-Cl})_{0.18}]$[a]	$[^nPr_4N]_2[Co^{II}_2H_4\mathbf{P^{iPr}buam}(\mu\text{-1,3-OC(NH)CH}_3)_{0.90}(Cl)_{0.10}]\cdot$DMA[b]	$[^nPr_4N]_2[Co^{II}_2H_4\mathbf{P^{tBu}buam}(\mu\text{-1,3-OC(NH)CH}_3)]\cdot$DMA	$[^nPr_4N]_2[Co^{II}_2H_4\mathbf{P^{iPr}buam}(\mu\text{-1,3-OAc})]\cdot$DMA	$[^nPr_4N]_2[Co^{II}_2H_4\mathbf{P^{tBu}buam}(\mu\text{-1,3-OAc})]\cdot$DMA	$K_2[Co^{II}H_2\mathbf{P^{tBu}uam}(OH)]\cdot$2DMA
molecular formula	$C_{53}H_{109.82}Co_2N_{14}O_{4.82}Cl_{0.18}$	$C_{58.8}H_{121.6}Co_2N_{15.9}O_{5.9}Cl_{0.10}$	$C_{63}H_{130}Co_2N_{16}O_6$	$C_{59}H_{121}Co_2N_{15}O_7$	$C_{63}H_{129}Co_2N_{15}O_7$	$C_{30}H_{59}CoK_2N_9O_5$
fw	1141.41	1269.59	1325.69	1270.57	1326.67	762.99
T (K)	100(2)	100(2)	100(2)	100(2)	100(2)	100(2)
space group	$P\bar{1}-C_i^1$ (No. 2)	$P2_1/n$	$Cc-C_s^4$	$P2_1/n$	$P2_1/n$	$P2_1/c-C_{2h}^5$ (No. 14)
a (Å)	11.647(1)	11.707(3)	13.562(1)	11.310(4)	13.5403(12)	11.137(4)
b (Å)	12.429(1)	26.956(8)	19.052(2)	28.068(9)	18.9521(16)	16.708(6)
c (Å)	23.566(2)	22.901(6)	29.098(2)	22.372(7)	29.080(2)	21.762(8)
α (deg)	96.208(4)	90	90	90	90	90
β (deg)	93.471(4)	101.976(7)	92.625(3)	92.779(9)	92.144(4)	100.683(6)
γ (deg)	107.709(4)	90	90	90	90	90
Z	2 ($Z' = 1$)	4 ($Z' = 1$)	4 ($Z' = 0.5$)	4 ($Z' = 1$)	4 ($Z' = 1$)	4 ($Z' = 1$)
V (Å^3)	3215.1(5)	7070(3)	7511(1)	7094(4)	7457.2(10)	3979(2)
δ_{calcd} (Mg/m^3)	1.182	1.191	1.158	1.190	1.104	1.274
R[c]	0.054	0.047	0.062	0.055	0.047	0.0426
R_w[d]	0.139	0.126	0.179	0.155	0.137	0.1203
GOF[e]	0.978	1.050	1.036	1.030	1.073	1.003

[a] This salt cocrystallized with 18.2% of the isodimensional anion $[Co^{II}_2H_4\mathbf{P^{iPr}buam}(\mu\text{-Cl})]^{2-}$. [b] This salt cocrystallized with 10% of the isodimensional anion $[Co^{II}_2H_4\mathbf{P^{iPr}buam}(Cl)]^{2-}$. [c] $R = [\sum|\Delta F|/\sum|F_o|]$. [d] $R_w = \{\sum[w(F_o^2 - F_c^2)^2]/\sum[w(F_o^2)^2]\}^{1/2}$. [e] Goodness of fit on F^2.

eter with a high-performance liquid chromatography (HPLC; HP 1050) HP particle-beam interface mass system and a phasor FAB gun. FAB experiments were carried out in a thioglycerol/glycerol matrix, and a xenon fast atom beam was used. Electrospray ionization (ESI) mass spectra were recorded on a Micromass LCT Premier spectrometer operating in W mode (high- and low-resolution modes). Melting points were obtained with a Laboratory Devices MEL-TEMP apparatus and are uncorrected. FTIR spectra were collected on a Mattson Genesis series FTIR instrument with values reported in wavenumbers. Electronic spectra were collected on a Cary 50 spectrophotometer using 1.00 mm or 1.00 cm quartz cuvettes. Room temperature magnetic susceptibility measurements of solid samples were obtained using a MSB-1 magnetic susceptibility balance (Johnson Matthey). Perpendicular-mode X-band electron paramagnetic resonance (EPR) spectra were collected using a Bruker EMX spectrometer equipped with an ER041XG microwave bridge. A quartz liquid-nitrogen finger Dewar (Wilmad Glass) was used to record spectra at 77 K, and 4 K spectra were obtained using an Oxford Instrument liquid-helium quartz cryostat. Spectra for EPR-active samples were collected using the following spectrometer settings: attenuation = 15 dB, microwave power = 6.300 mW, frequency = 9.26 GHz, sweep width = 5000 G, modulation amplitude = 10.02 G, gain = 1.00×10^3, conversion time = 81.920 ms, time constant = 655.36 ms, and resolution = 1024 points.

Crystallographic Methods. Partial crystallographic data for $[^nPr_4N]_2[Co^{II}_2H_4\mathbf{P^{iPr}buam}(\mu\text{-OH})]$, $[^nPr_4N]_2[Co^{II}H_4\mathbf{P^{R}buam}(\mu\text{-1,3-OC(NH)CH}_3)]\cdot$DMA, $[^nPr_4N]_2[Co^{II}H_4\mathbf{P^{R}buam}(\mu\text{-1,3-OAc})]\cdot$DMA, and $K_2[Co^{II}H_4\mathbf{P^{tBu}uam}(OH)]\cdot$2DMA are presented in Table 1. Note that $[^nPr_4N]_2[Co^{II}_2H_4\mathbf{P^{iPr}buam}(\mu\text{-OH})]$ and $[^nPr_4N]_2[Co^{II}_2H_4\mathbf{P^{iPr}buam}(\mu\text{-1,3-OC(NH)CH}_3)]\cdot$DMA cocrystallized with 18.2% and 10.0% of the isodimensional anion $[Co^{II}_2H_4\mathbf{P^{iPr}buam}(\mu\text{-Cl})]^{2-}$. Details of the data collection and refinement for each structure, plus full refinement parameters in CIF format, are found in the Supporting Information.

Scheme 1. Preparative Route for $[Co^{II}_2H_4\mathbf{P^{R}buam}(\mu\text{-OH})]^{2-}$ [a]

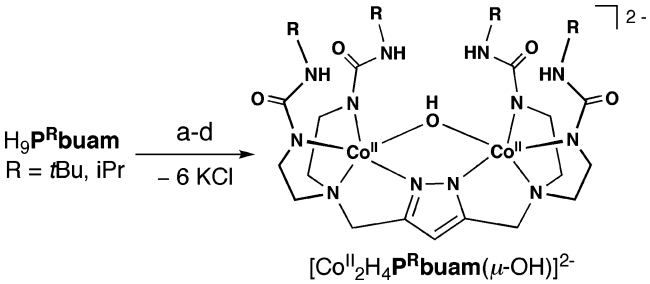

[a] Conditions: (a) 6 equiv of KH, DMA, rt, Ar; (b) 2 equiv of $CoCl_2$, DMA, rt, Ar; (c) 1 equiv of H_2O, DMA, rt, Ar; (d) 2 equiv of $[^nPr_4N]Cl$, DMA, rt, Ar.

Results and Discussion

Preparation and Spectroscopic Properties of the $[^nPr_4N]_2[Co^{II}_2H_4P^{R}buam(\mu\text{-OH})]$ Complexes. Preparation of the hydroxo-bridged dimers was accomplished by following the method outlined in Scheme 1. Treating the binucleating ligands with 6 equiv of KH affords $[H_3\mathbf{P^{R}buam}]^{6-}$ in DMA, which readily binds two Co ions to produce $[Co^{II}_2H_3\mathbf{P^{R}buam}]^{2-}$. Without isolation, $[Co^{II}_2H_3\mathbf{P^{R}buam}]^{2-}$ was treated with 1 equiv of H_2O to form the $[Co^{II}_2H_4\mathbf{P^{R}buam}(\mu\text{-OH})]^{2-}$ complexes, which were metathesized with 2 equiv of $[^nPr_4N]Cl$ to afford $[^nPr_4N]_2[Co^{II}_2H_4\mathbf{P^{R}buam}(\mu\text{-OH})]$ in yields greater than 94%. Normally, 5 equiv of base are used to bind two metal ions to these ligands; the extra 1 equiv of base deprotonates one of the α′NH groups to provide complexes with an additional basic site within the cavity. This is needed to act as an internal base to scavenge the proton produced when the hydroxide ion is formed from water. A similar synthetic method has been used to prepare M−OH complexes with tripodal urea ligands.[11] Analytical and spectroscopic measurements of the $[^nPr_4N]_2[Co^{II}_2H_4\mathbf{P^{R}buam}(\mu\text{-}$

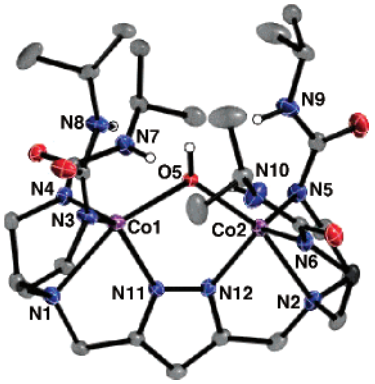

Figure 3. Molecular structure of $[Co^{II}_2H_4\mathbf{P^{iPr}buam}(\mu\text{-OH})]^{2-}$. The ellipsoids are drawn at the 50% probability level, and C-bonded H atoms are omitted for clarity.

OH)] salts indicated that the products isolated directly from the reaction mixtures were of sufficient purity to be used for further studies.

The FTIR spectra of both the ^{i}Pr and ^{t}Bu derivatives show weak peaks at 3612 and 3620 cm^{-1} that are assigned to the M(O−H) vibrations (Figure S1A in the Supporting Information). The NH region indicates that the ^{i}Pr analogue contains more of a symmetric arrangement of H-bond donors, giving a single sharp peak. In contrast, the ^{t}Bu derivative has two separate N−H peaks, suggesting a less symmetrical arrangement of H-bond donors. Similar vibrational properties were observed for the previously reported chloro analogues, $[Co^{II}_2H_4\mathbf{P^{R}buam}(\mu\text{-Cl})]^{2-}$, in which the ^{i}Pr derivative possessed a more symmetric H-bonding network about the chloro ligand compared to the ^{t}Bu analogue.[12] Both $[Co^{II}_2H_4\mathbf{P^{R}buam}(\mu\text{-OH})]^{2-}$ complexes exhibit similar optical properties in solution (Figure S1B in the Supporting Information).

Solid-State Structure of $[^n\mathrm{Pr_4N}]_2[Co^{II}_2H_4\mathbf{P^{iPr}buam}(\mu\text{-OH})]$. X-ray-quality single crystals of $[^n\mathrm{Pr_4N}]_2[Co^{II}_2H_4\mathbf{P^{iPr}buam}(\mu\text{-OH})]$ were obtained by vapor diffusion of diethyl ether into a DMA solution of the isolated metal salt, which were stable for weeks under a dry, anaerobic environment. Crystals of $[^n\mathrm{Pr_4N}]_2[Co^{II}_2H_4\mathbf{P^{tBu}buam}(\mu\text{-OH})]$ were obtained in the same manner but were not suitable to obtain a molecular structure by X-ray diffraction. The molecular structure of the isopropyl derivative determined from X-ray diffraction data is presented in Figure 3, with selected distances and angles shown in Table 2. The structure reveals the Co^{II} centers as five-coordinate with distorted trigonal-bipyramidal geometry. A single hydroxo ligand that bridges between the two Co^{II} ions is present in the complex, producing a metal−metal separation of 3.5857(5) Å. The $Co^{II}-\mu$-OH−Co^{II} unit is statistically symmetrical, having Co1−O5 and Co2−O5 distances of 2.128(4) and 2.133(4) Å. These Co^{II}−OH distances are significantly longer compared to the average distance observed for other reported synthetic $Co^{II}-\mu$-OH−Co^{II} compounds [avg Co^{II}−O(H) = 2.004 Å].[18] Other distortions away from trigonal-bipyramidal coordination geometry presumably occur to accommodate the $Co^{II}-\mu$-OH−Co^{II} unit. For instance, the N1−Co1−O5 and N2−Co2−O5 angles are less than 162°, significantly reduced from the normally observed angle of 180°. In addition, the Co1−N1 and Co2−N2 distances of 2.372(2) and 2.394(2) Å are 0.16 Å longer from those observed in $[Co^{II}_2H_4\mathbf{P^{iPr}buam}(\mu\text{-Cl})]^{2-}$, the related $Co^{II}-\mu$-Cl−Co^{II} complex.

Table 2. Selected Bond Distances (Å) and Angles (deg) for $[Co^{II}_2H_4\mathbf{P^{iPr}buam}(\mu\text{-OH})]^{2-}$

Co1−N1	2.372(2)	N3−Co1−N1	80.8(1)
Co1−N3	2.002(2)	N4−Co1−N1	79.1(1)
Co1−N4	1.988(2)	N11−Co1−N1	73.5(1)
Co1−N11	1.992(2)	N5−Co2−N6	113.3(1)
Co2−N2	2.394(2)	N5−Co2−N12	118.2(1)
Co2−N5	1.980(2)	N6−Co2−N12	115.8(1)
Co2−N6	1.984(2)	N5−Co2−N2	78.9(1)
Co2−N12	1.970(2)	N6−Co2−N2	81.2(1)
Co1−O5	2.128(4)	N12−Co2−N2	73.8(1)
Co2−O5	2.133(4)	N3−Co1−O5	111.8(1)
Co1···Co2	3.5857(5)	N4−Co1−O5	107.1(1)
N7···O5	3.213(5)	N11−Co1−O5	87.2(1)
N8···O5	3.201(5)	N1−Co1−O5	160.1(1)
N9···O5	3.327(5)	N5−Co2−O5	107.1(1)
N10···O5	3.116(5)	N6−Co2−O5	111.0(1)
N3−Co1−N4	116.0(1)	N12−Co2−O5	88.2(1)
N3−Co1−N11	112.5(1)	N2−Co2−O5	161.6(1)
N4−Co1−N11	118.3(1)	Co1−O5−Co2	114.6(2)

The molecular structure of $[Co^{II}_2H_4\mathbf{P^{iPr}buam}(\mu\text{-OH})]^{2-}$ also reveals that the four α′NH groups are positioned within the cavity toward the bridging HO^- ligand. There may be some dipolar effect resulting from the presence of four H-bond donors proximal to the $Co^{II}-\mu$-OH−Co^{II} unit, which could contribute to the relatively long Co−O5 bonds. However, all of the α′N···O5 distances are greater than 3.11 Å; these distances are too long for H-bonds, which are generally less than 3.0 Å.[19] The placement of the hydroxo ligand within the cavity is such that intramolecular H-bonds to the rigid urea group are diminished. Note that in other complexes of $[H_4\mathbf{P^{iPr}buam}]^{5-}$, such as $[Co^{II}_2H_4\mathbf{P^{iPr}buam}(\mu\text{-Cl})]^{2-}$, multiple intramolecular H-bonds are observed between the α′NH groups and the chloro bridge. A comparison of the molecular structures of the $Co^{II}-\mu$-X−Co^{II} (X = OH^-, Cl^-) complexes reveals that the chloro ligand is nearly 0.5 Å farther from the Co−Co axis than O5, placing the bridging Cl ion in an optimal position to form H-bonds.

Hydration of Acetonitrile and Hydrolysis of Ethyl Acetate with $[Co^{II}_2H_4\mathbf{P^{R}buam}(\mu\text{-OH})]^{2-}$. During the course of our studies on $[Co^{II}_2H_4\mathbf{P^{R}buam}(\mu\text{-OH})]^{2-}$, we discovered that it hydrates acetonitrile to form complexes with bridging μ-1,3-acetamidato ligands (μ-1,3-OC(NH)CH_3; Scheme 2). The reactions were completed within 2 h at room temperature, and crystalline products were obtained by vapor diffusion of diethyl ether into acetonitrile solutions of the $[Co^{II}_2H_4\mathbf{P^{R}buam}(\mu\text{-OH})]^{2-}$ complexes: $[^n\mathrm{Pr_4N}]_2[Co^{II}_2H_4\mathbf{P^{tBu}buam}(\mu\text{-1,3-OC(NH)CH}_3)]\cdot$DMA and $[^n\mathrm{Pr_4N}]_2[Co^{II}_2H_4\mathbf{P^{iPr}buam}(\mu\text{-1,3-OC(NH)CH}_3)]\cdot$DMA were obtained in 60% and 77% crystalline yields, respectively.

(18) (a) Kitajima, N.; Hikichi, S.; Taniaka, M.; Moro-oka, Y. *J. Am. Chem. Soc.* **1993**, *115*, 5496−5508. (b) He, C.; Lippard, S. J. *J. Am. Chem. Soc.* **1998**, *120*, 105−113. (c) Singh, U. P.; Babbar, P.; Sharma, A. K. *Inorg. Chim. Acta* **2005**, *358*, 271−278.

(19) (a) Jeffrey, G. A. *An Introduction to Hydrogen Bonding*; Oxford University Press, Inc.: New York, 1997. (b) Desiraju, G. R.; Steiner, T. *The Weak Hydrogen Bond In Structural Chemistry and Biology*; Oxford University Press Inc.: New York, 1999.

Scheme 2. Hydration/Hydrolysis Reactions with $[Co^{II}_2H_4\mathbf{P^R buam}(\mu\text{-OH})]^{2-}$

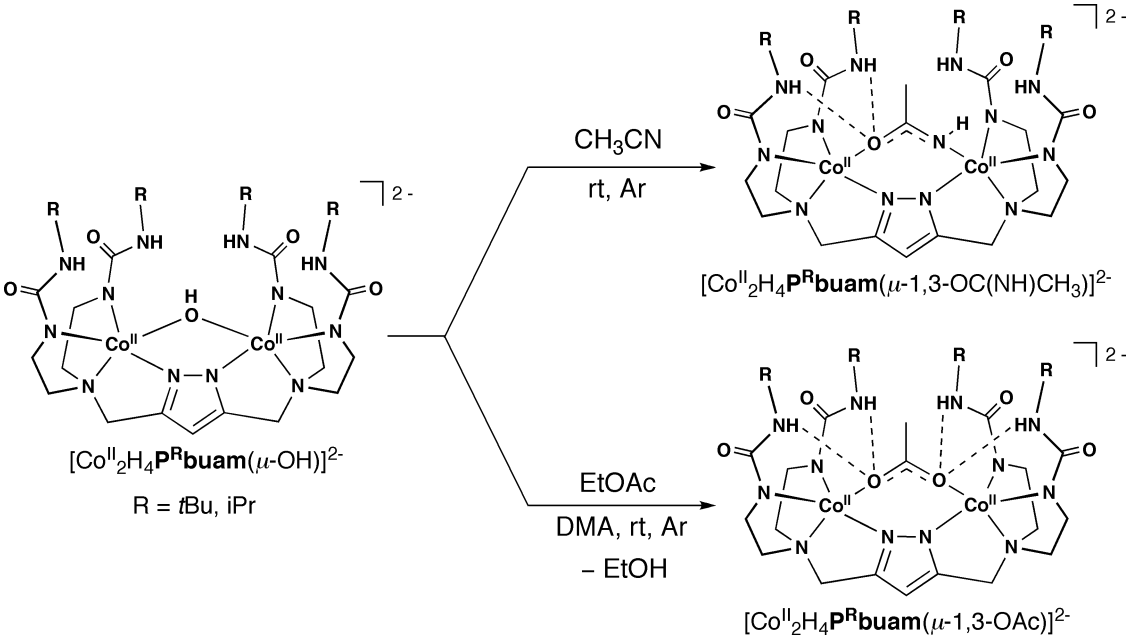

The vibrational properties of the isolated salts are consistent with the formation of acetamidato ligands.[20] The signature M(O−H) stretching for the bridging hydroxo complexes at $\nu \sim 3620$ cm^{-1} was absent in the solid-state FTIR spectra of the crystallized products. Two new carbonyl-type peaks appeared at $\nu = 1538$ and 1494 cm^{-1} (R = ^{i}Pr) and at $\nu = 1539$ and 1516 cm^{-1} (R = ^{t}Bu). In addition, a new weak, but relatively sharp, ν(NH) band was present at 3415 cm^{-1} for R = ^{i}Pr and at 3406 cm^{-1} for R = ^{t}Bu (Figure S2 in the Supporting Information).

While exploring the scope of hydrolysis performed by $[Co^{II}_2H_4\mathbf{P^R buam}(\mu\text{-OH})]^{2-}$, it was also found that inactivated esters such as ethyl acetate can be cleaved (Scheme 2). Dissolving $[^n Pr_4N]_2[Co^{II}_2H_4\mathbf{P^R buam}(\mu\text{-OH})]$ in a 1:1 solution of DMA and ethyl acetate and stirring the mixture for 2 h at room temperature under argon produced complexes with μ-1,3-acetate ligands. The isolated salts were crystallized in a 1:1 mixture of DMA and ethyl acetate using diethyl ether vapor diffusion, affording $[^n Pr_4N]_2[Co^{II}_2H_4\mathbf{P^{tBu} buam}(\mu\text{-1,3-OAc})]\cdot$DMA and $[^n Pr_4N]_2[Co^{II}_2H_4\mathbf{P^{iPr} buam}(\mu\text{-1,3-OAc})]\cdot$DMA in 68% and 79% crystalline yield, respectively.

The isolated complexes had predictable changes in the their spectral properties that indicated the presence of acetate bridges. The FTIR spectra again showed the absence of peaks associated with an M(O−H) vibration from the starting μ-hydroxo compounds, and the signals associated with NH vibrations changed from a cluster of medium-intensity, broad peaks to a single, strong, and sharp peak, indicating a different H-bonding network within the cavities (Figure S3A in the Supporting Information). The solid-state FTIR spectra of the crystalline products show distinctive symmetric and asymmetric stretching vibrations consistent with a μ-1,3-OAc moiety at ν_a(COO) = 1553 cm^{-1} and ν_s(COO) = 1407 cm^{-1} for $[Co^{II}_2H_4\mathbf{P^{tBu} buam}(\mu\text{-1,3-OAc})]^{2-}$ and at ν_a(COO) = 1561 cm^{-1} and ν_a(COO) = 1411 cm^{-1} for the ^{i}Pr derivative (Figure S3B in the Supporting Information). The $\Delta\nu$ values ($\Delta\nu$ = 146 cm^{-1} for R = ^{t}Bu and $\Delta\nu$ = 150 cm^{-1} for R = ^{i}Pr) are in agreement with the literature values found for other complexes with μ-1,3 acetate bridges.[21]

Direct Preparations of Hydration/Hydrolysis Products. To confirm the formulation of the hydration/hydrolysis products, direct synthetic methods were developed for complexes with Co^{II}−(μ-1,3-X′)−Co^{II} (X′ = OAc$^-$, [OC(NH)CH$_3$]$^-$) cores. The procedures were modeled after that used to prepare the $[Co^{II}_2H_4\mathbf{P^R buam}(\mu\text{-OH})]^{2-}$ complexes and are outlined in Scheme 3. Tetrapropylammonium salts of the $[Co^{II}_2H_4\mathbf{P^R buam}(\mu\text{-1,3-X′})]^{2-}$ complexes were isolated in nearly quantitative yields and displayed spectral properties identical with those of the crystallized products obtained from the hydration/hydrolysis reactions.

Molecular Structures of $[Co^{II}_2H_4\mathbf{P^R buam}(\mu\text{-1,3-X′})]^{2-}$. $[Co^{II}_2H_4\mathbf{P^R buam}(\mu\text{-1,3-OC(NH)CH_3})]^{2-}$ Complexes. X-ray-quality crystals of $[^n Pr_4N]_2[Co^{II}_2H_4\mathbf{P^R buam}(\mu\text{-1,3-OC(NH)CH}_3)]$ and $[^n Pr_4N]_2[Co^{II}_2H_4\mathbf{P^R buam}(\mu\text{-1,3-OAc})]$ were obtained by vapor diffusion of diethyl ether into DMA solutions of the appropriate isolated metal salt. These salts were stable for weeks under a dry, anaerobic environment. Single-crystal X-ray diffraction measurements corroborate the similarities in the solid-state structures for both $[Co^{II}_2H_4\mathbf{P^R buam}(\mu\text{-1,3-OC(NH)CH}_3)]^{2-}$ complexes. The molecular structure of the ^{i}Pr derivative is presented in Figure 4, with selected metrical parameters for both complexes found in Table 3. The acetamidato H atom in $[Co^{II}_2H_4\mathbf{P^{iPr} buam}(\mu\text{-1,3-OC(NH)CH}_3)]^{2-}$ was located and refined, and the different O5−C30 and N13−C30 bond lengths of 1.281(2) and 1.310(3) Å confirms the presence of an acetamidato ligand. The ^{t}Bu analogue contained a disordered acetamidato ligand with nearly equally occupied

(20) Meyer, F.; Kaifer, E.; Kircher, P.; Heinze, K.; Pritzkow, H. *Chem.*−*Eur. J.* **1999**, *5*, 1617−1630.

(21) Nakamoto, K. *Infrared and Raman Spectra of Inorganic and Coordination Compounds*, 5th ed.; John Wiley: New York, 1997.

Scheme 3. Preparative Routes for $[Co^{II}_2H_4\mathbf{P^R buam}(\mu\text{-}1,3\text{-}X')]^{2-}$ ($X' = OAc^-$, $[OC(NH)CH_3]^-$)[a]

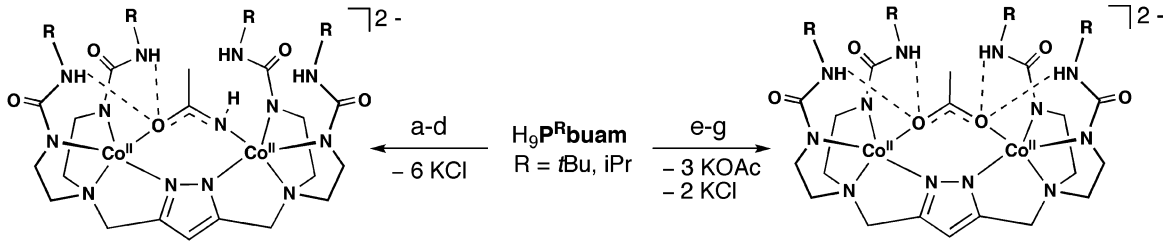

$[Co^{II}_2H_4\mathbf{P^R buam}(\mu\text{-}1,3\text{-}OC(NH)CH_3)]^{2-}$ $[Co^{II}_2H_4\mathbf{P^R buam}(\mu\text{-}1,3\text{-}OAc)]^{2-}$

[a] Conditions: (a) 6 equiv of KH, DMA, rt, Ar; (b) 2 equiv of $CoCl_2$, DMA, rt, Ar; (c) 1 equiv of acetamide, DMA, rt, Ar; (d) 2 equiv of $[^nPr_4N]Cl$, DMA, rt, Ar; (e) 5 equiv of KH, DMA, rt, Ar; (f) 2 equiv of $Co(OAc)_2$, DMA, rt, Ar; (g) 2 equiv of $[^nPr_4N]Cl$, DMA, rt, Ar.

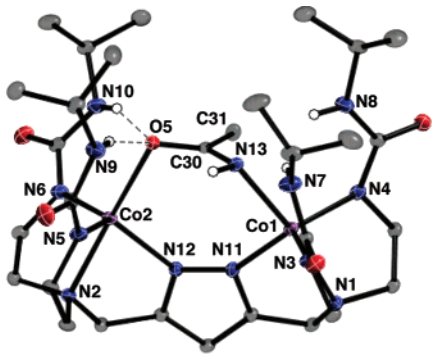

Figure 4. Molecular structure of $[Co^{II}_2H_4\mathbf{P^{iPr}buam}(\mu\text{-}1,3\text{-}OC(NH)CH_3)]^{2-}$. The ellipsoids are drawn at the 50% probability level, and C-bonded H atoms are omitted for clarity.

(52/48) orientations about the pseudo-C_2 axis of the dianion (Figure S6 in the Supporting Information). In addition, the H atom on N13 of the acetamidate in $[Co^{II}_2H_4\mathbf{P^{tBu}buam}(\mu\text{-}1,3\text{-}OC(NH)CH_3)]^{2-}$ could not be located in the Fourier difference map. Nevertheless, large differences in bond lengths were found within the bridging ligand to support the presence of both C−O and C−N bonds [i.e., 1.171(10) and 1.448(10) Å].

Each complex contains Co centers that are five-coordinate with distorted trigonal-bipyramidal geometry containing a deprotonated acetamidato as a bridge between the two metal centers. The Co1···Co2 separations are 4.482(1) Å for the ^{i}Pr analogue and 4.6697(5) Å for the ^{t}Bu analogue; these distances are nearly 1.0 Å longer than those in the μ-hydroxo complex, illustrating the flexibility within the $[H_4\mathbf{P^R buam}]^{5-}$ ligands about the pyrazolate core. In $[Co^{II}_2H_4\mathbf{P^{iPr}buam}(\mu\text{-}1,3\text{-}OC(NH)CH_3)]^{2-}$, the H-bond donors of the urea groups form intramolecular H-bonds with the heteroatoms of the acetamidato bridge (Table 3). The average α′N···OC(NH)-CH_3 and α′N···NHC(O)CH_3 distances of 2.800(2) and 3.034-(2) Å are within those normally observed for H-bonds; in addition, N−H···X (X = O, N) angles greater than 140° are observed, which are consistent with intramolecular H-bonds.[19]

Note the unusual binding of the bridging acetamidato, in which the C−C bond is nearly perpendicular to the pyrazolate plane (Figure 4). To compare this structural feature to other bridging systems, a reference mean plane was defined by the two metal centers and the atom(s) of the bridging ligand bound directly to the metal centers. For instance, in $[Co^{II}_2H_4\mathbf{P^{iPr}buam}(\mu\text{-}1,3\text{-}OC(NH)CH_3)]^{2-}$, the

Table 3. Selected Bond Distances (Å) and Angles (deg) for $[Co^{II}_2H_4\mathbf{P^R buam}(\mu\text{-}1,3\text{-}OC(NH)CH_3)]^{2-}$ (R = ^{i}Pr and ^{t}Bu)

	R	
	^{i}Pr	^{t}Bu
Co1−N1	2.204(1)	2.191(4)
Co1−N3	2.022(1)	1.996(5)
Co1−N4	2.018(1)	2.018(5)
Co1−N11	2.128(1)	2.165(5)
Co2−N2	2.181(1)	2.173(5)
Co2−N5	2.028(2)	2.034(5)
Co2−N6	2.001(1)	2.006(5)
Co2−N12	2.088(1)	2.120(5)
Co2−O5	2.128(1)	2.103(5)
Co1−N13	2.105(2)	2.096(5)
Co1···Co2	4.482(1)	4.6697(5)
N9···O5	2.770(2)	2.916(7)
N10···O5	2.830(2)	2.897(7)
N7···N13	3.048(2)	2.875(8)
N8···N13	3.020(2)	2.913(8)
N3−Co1−N4	3.048(2)	114.6(2)
N3−Co1−N11	110.88(6)	116.21(19)
N4−Co1−N11	119.30(5)	120.60(18)
N3−Co1−N1	120.67(5)	81.94(17)
N4−Co1−N1	81.13(5)	80.80(17)
N11−Co1−N1	77.08(5)	77.95(17)
N5−Co2−N6	120.02(6)	113.2(2)
N5−Co2−N12	117.96(5)	121.7(2)
N6−Co2−N12	113.20(5)	117.0(2)
N5−Co2−N2	80.61(6)	81.27(19)
N6−Co2−N2	81.46(6)	80.88(18)
N12−Co2−N2	77.94(5)	79.25(18)
N5−Co2−O5	97.89(5)	98.9(2)
N6−Co2−O5	101.96(5)	104.60(19)
N12−Co2−O5	100.16(5)	121.7(2)
N2−Co2−O5	176.56(5)	173.8(2)
N3−Co1−N13	105.73(6)	104.6(2)
N4−Co1−N13	102.75(6)	99.60(19)
N11−Co1−N13	92.51(6)	95.5(2)
N1−Co1−N13	169.41(6)	172.41(19)

atoms Co2, O5, N13, and Co1 were used to define the reference mean plane. The fold angle was then determined, which is the angle between the reference mean plane and the plane containing atoms of the bridging ligand: in the ^{i}Pr complex, the ligand plane contains the atoms of the acetamidato bridge, O5, N13, C30, and C31. Therefore, the fold angle observed for the bridging acetamidato is 63° in $[Co^{II}_2H_4\mathbf{P^{iPr}buam}(\mu\text{-}1,3\text{-}OC(NH)CH_3)]^{2-}$ and 84° in $[Co^{II}_2H_4\mathbf{P^{tBu}buam}(\mu\text{-}1,3\text{-}OC(NH)CH_3)]^{2-}$. Other bridging amidate complexes have fold angles that are usually less than 20°.[20,22,23]

The larger fold angles in the $[Co^{II}_2H_4\mathbf{P^R buam}(\mu\text{-}1,3\text{-}OC(NH)CH_3)]^{2-}$ complexes undoubtedly arise from secondary coordination sphere effects created by the $[H_4\mathbf{P^R buam}]^{5-}$

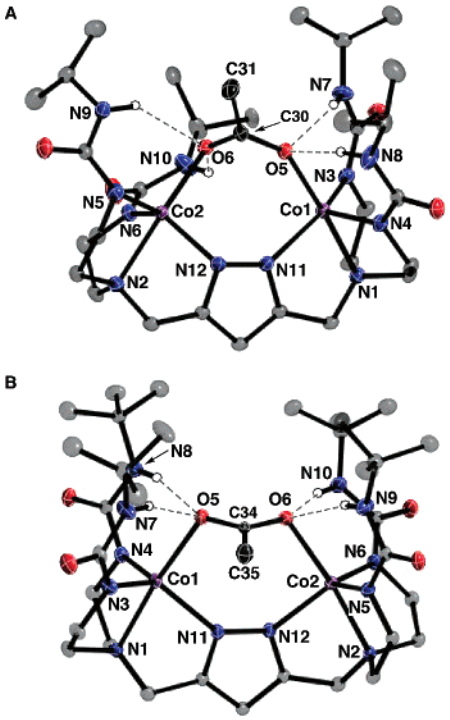

Figure 5. Molecular structures of [Co$^{II}_2$H$_4$**P^{R}buam**(μ-1,3-OAc)]$^{2-}$: R = ^{i}Pr (A) and ^{t}Bu (B). The ellipsoids are drawn at the 50% probability level, and non-urea H atoms are omitted for clarity.

ligand. Optimal intramolecular H-bonds occur when electronic repulsions are minimized between the N−H bond of the deprotonated acetamidate and the H-bond donors within the cavity; this occurs when the fold angle is large. Additionally, steric repulsions with the bulky R groups appended to the urea arms can influence the orientation of the bridging ligand, particularly in the ^{t}Bu derivative.

Molecular Structures of [Co$^{II}_2$H$_4$P^{R}buam(μ-1,3-OAc)]$^{2-}$. The solid-state molecular structures of [Co$^{II}_2$H$_4$**P^{R}buam**(μ-1,3-OAc)]$^{2-}$ are shown in Figure 5, with selected bond distances and angles presented in Table 4. The complexes also have Co centers with distorted trigonal-bipyramidal geometries containing an acetate ion as the bridging, external ligand. The Co1···Co2 separations are 4.311(1) and 4.6507(5) Å for [Co$^{II}_2$H$_4$**P^{iPr}buam**(μ-1,3-OAc)]$^{2-}$ and [Co$^{II}_2$H$_4$**P^{tBu}buam**(μ-1,3-OAc)]$^{2-}$, respectively. The metal−metal separation for the ^{t}Bu complex is comparable to that observed in the analogous bridging acetamidato complex; however, the ^{i}Pr complex exhibits a significantly shorter Co1···Co2 distance, which may be caused by the orientation of the bridging acetate (vide infra). The Co^{II}−O bond lengths for each complex are approximately 0.07 Å longer than the average Co^{II}−O bond distance reported for other Co^{II} dimers with bridging acetate ligands.[24] The lengthening of the Co^{II}−O bond is partially attributed to the intramolecular H-bonds between the [H$_4$**P^{R}buam**]$^{5-}$ ligands and the bridged acetate moieties.

Table 4. Selected Bond Distances (Å) and Angles (deg) for [Co$^{II}_2$H$_4$**P^{R}buam**(μ-1,3-OAc)]$^{2-}$ (R = ^{i}Pr, ^{t}Bu)

	R	
	^{i}Pr	^{t}Bu
Co1−N1	2.221(2)	2.178(16)
Co1−N3	2.017(2)	2.016(18)
Co1−N4	2.016(2)	2.008(17)
Co1−N11	2.066(2)	2.131(17)
Co2−N2	2.260(2)	2.163(16)
Co2−N5	2.024(2)	1.997(17)
Co2−N6	1.982(2)	2.027(17)
Co2−N12	2.038(2)	2.111(16)
Co1−O5	2.126(1)	2.139(14)
Co2−O6	2.112(2)	2.130(14)
Co1···Co2	4.311(1)	4.6507(5)
N7···O5	2.824(2)	2.915(3)
N8···O5	2.961(2)	2.937(2)
N9···O6	3.077(2)	2.920(2)
N10···O6	2.915(3)	2.943(3)
N3−Co1−N4	111.55(7)	113.74(7)
N3−Co1−N11	113.54(7)	119.96(7)
N4−Co1−N11	125.44(7)	118.92(7)
N3−Co1−N1	81.28(7)	81.95(7)
N4−Co1−N1	80.52(7)	81.39(7)
N11−Co1−N1	77.58(7)	81.82(7)
N5−Co2−N6	82.47(7)	115.34(7)
N5−Co2−N12	124.83(7)	117.11(7)
N6−Co2−N12	112.65(7)	119.50(7)
N5−Co2−N2	80.18(7)	81.40(7)
N6−Co2−N2	82.47(7)	80.84(7)
N12−Co2−N2	79.70(7)	79.23(6)
N3−Co1−O5	100.28(7)	99.67(6)
N4−Co1−O5	102.47(7)	103.44(6)
N11−Co1−O5	98.16(6)	94.46(6)
N1−Co1−O5	175.72(6)	173.12(6)
N5−Co2−O6	99.26(7)	103.77(6)
N6−Co2−O6	100.10(7)	100.59(6)
N12−Co2−O6	98.58(7)	94.35(6)
N2−Co2−O6	177.33(6)	173.18(6)

The molecular structures also reveal H-bonding networks surrounding the Co^{II}−μ-1,3−OAc−Co^{II} unit, involving the α′NH groups of [H$_4$**P^{R}buam**]$^{5-}$ and the O atoms of the bridging acetate. For [Co$^{II}_2$H$_4$**P^{tBu}buam**(μ-1,3-OAc)]$^{2-}$, all of the α′N···O distances are nearly equivalent at distances of less than 3.0 Å and N−H···O angles greater than 160°. A less symmetrical H-bonding network is found in the ^{i}Pr derivative, yet the α′N···O distances and angles also suggest the presence of four intramolecular H-bonds. The most noticeable difference between the structures of the two complexes is the orientation of the acetate bridge. In [Co$^{II}_2$H$_4$**P^{iPr}buam**(μ-1,3-OAc)]$^{2-}$, the C30−C31 vector is nearly parallel to the pyrazolate plane, whereas the comparable bond in the ^{t}Bu analogue, the C34−C35 vector, is virtually perpendicular to the pyrazolate plane. This difference is seen in their fold angles, which are 34° (R = ^{i}Pr) and 82° (R = ^{t}Bu). The small fold angle in [Co$^{II}_2$H$_4$**P^{iPr}buam**(μ-1,3-OAc)]$^{2-}$ is similar to those found in other complexes with bridging acetates and occurs because the appended ^{i}Pr groups create a relatively open cavity that can accommodate the C30−C31 vector. In contrast, the more sterically demanding ^{t}Bu groups in [Co$^{II}_2$H$_4$**P^{tBu}buam**(μ-1,3-OAc)]$^{2-}$ form a constrained structure, without enough space to house the methyl group of the bridging acetate. Conse-

(22) (a) Curtis, N. J.; Hagen, K. S.; Sargeson, A. M. *J. Chem. Soc., Chem. Commun.* **1984**, 1571−1573. (b) Alcock, N. W.; Creaser, I. I.; Curtis, N. J.; Roecker, L.; Sargeson, A. M.; Willis, A. C. *Aust. J. Chem.* **1990**, *43*, 643−654.
(23) Bauer, C. B.; Concolino, T. E.; Eglin, J. L.; Rogers, R. D.; Staples, R. J. *J. Chem. Soc., Dalton Trans.* **1998**, 2813−2817.
(24) Brown, D. A.; Errington, W.; Glass, W. K.; Haase, W.; Kemp, T. J.; Nimir, H.; Ostrovsky, S. M.; Werner, R. *Inorg. Chem.* **2001**, *40*, 5962−5971.

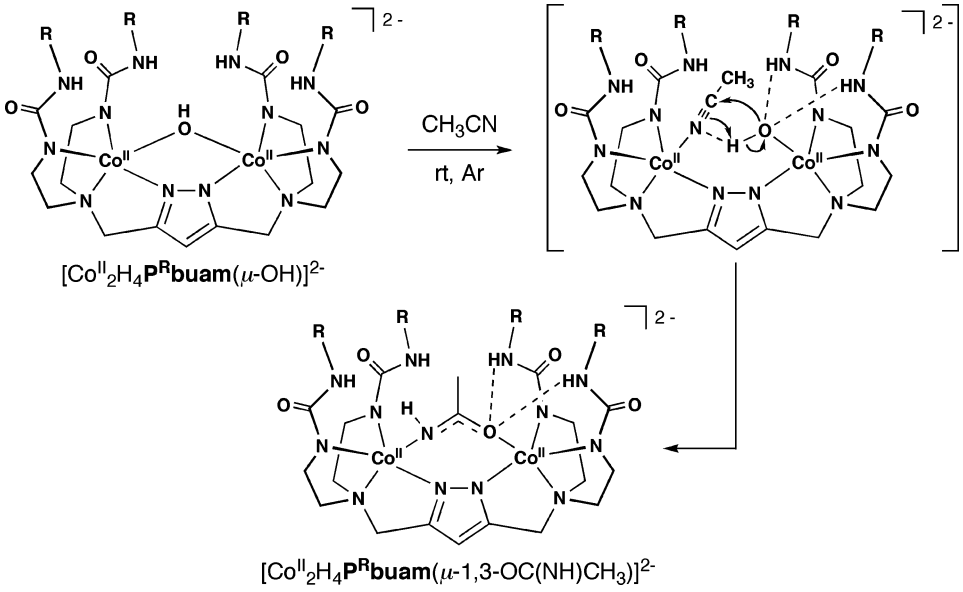

Figure 6. Proposed mechanism for the hydration of acetonitrile by $[Co^{II}_2H_4\mathbf{P^Rbuam}(\mu\text{-OH})]^{2-}$.

quently, the C34−C35 vector is positioned out of the cavity. These structural differences demonstrate that the R groups appended to the ends of the urea arms allow additional control of the secondary coordination sphere by regulating the size and shape of the H-bonding pocket.

Mechanism of Hydration/Hydrolysis. Outlined in Figure 6 is a proposed mechanism for the hydration of acetonitrile by $[Co^{II}_2H_4\mathbf{P^Rbuam}(\mu\text{-OH})]^{2-}$; this mechanism is based on other reported dinuclear systems that perform similar reactions.[20,22,23,25−27] Displacement of the hydroxo ligand from one of the Co centers by an N-coordinated nitrile results in a change in the coordination of the hydroxo ligand from a bridging mode to a terminal mode. This process may be facile and energetically favorable because of the H-bond donors, which can provide stabilization to the resulting terminal hydroxo intermediate. Binding the nitrile substrate places the now activated, electrophilic carbon atom in a position that allows intramolecular nucleophilic attack by the adjacent hydroxo ligand. A final proton shift produces the stable μ-1,3-acetamidato bridge. A similar mechanism would apply to the hydrolysis of ethyl acetate, producing the bridging acetate and ethanol.

A hydroxide or water spanning two metal ions has been detected crystallographically in many biological hydrolases and is normally considered the active nucleophile.[4] A tightly bound, bridging hydroxide would yet be expected to exhibit relatively low nucleophilic character. Thus, a shift in the binding mode of the bridging hydroxo ligand to a terminal position prior to attack on the coordinated substrate would be expected. This type of shift in the binding mode has been suggested by studies performed on aminopepidase, a dinuclear metallohydrolase.[28] In addition, secondary-sphere H-bonds are proposed to play an essential role in the enzymatic activity of many hydrolases.[5] We have shown that $[H_4\mathbf{P^Rbuam}]^{5-}$ provides H-bond donors capable of forming intramolecular H-bonds with species bound within the cavity;[12] thus, it is reasonable to suggest that the H-bond donors are playing a role in regulating the reactivity of $[Co^{II}_2H_4\mathbf{P^Rbuam}(\mu\text{-OH})]^{2-}$ while adding structural stability to the proposed reactive intermediate and final product.

Synthesis and Structure of a Monomeric Co^{II}−OH Complex. The mononuclear complex, $[Co^{II}H_2\mathbf{P^{tBu}uam}(OH)]^{2-}$, was prepared in order to explore the cooperation of two metal ions in the hydration/hydrolysis of substrates. We reasoned that the mononuclear Co^{II}−OH complex was a good system for comparison because it possesses properties similar to those of $[Co^{II}_2H_4\mathbf{P^Rbuam}(\mu\text{-OH})]^{2-}$ but can prevent interactions between two $[Co^{II}H_2\mathbf{P^{tBu}uam}(OH)]^{2-}$ complexes. Note that similar strategies were used by Meyer and Mareque-Rivas in probing metal-assisted hydrolytic transformations.[9,20] The ligand $[H_2\mathbf{P^{tBu}uam}]^{3-}$ was designed to represent half of the dinucleating ligand $[H_4\mathbf{P^{tBu}buam}]^{5-}$, in which a ^{t}Bu group replaces one set of urea arms (Figure 2). The syntheses of $H_5\mathbf{P^{tBu}uam}$ and its corresponding Co^{II}−OH complex are outlined in Scheme 4.

The molecular structure of $[Co^{II}H_2\mathbf{P^{tBu}uam}(OH)]^{2-}$, determined from single-crystal X-ray diffraction data, is presented in Figure 7, and metrical parameters are found in Table 5. The Co center is five-coordinate and has nearly perfect trigonal-bipyramidal geometry based on the angular structural parameter introduced by Addison et al.[29] The primary coordination sphere contains the same ligation as that observed for the Co ions in the dinuclear derivatives.

(25) (a) Hazell, A.; Jensen, K. B.; McKenzie, C. J.; Toftlund, H. *Inorg. Chem.* **1994**, *33*, 3127−3134. (b) Wilkinson, E. C.; Dong, Y.; Que, L., Jr. *J. Am. Chem. Soc.* **1994**, *116*, 8394−8395. (c) Duboc-Toia, C.; Menage, S.; Vincent, J.-M.; Averbuch-Pouchot, M. T.; Fontecave, M. *Inorg. Chem.* **1997**, *36*, 6148−6149.
(26) Frey, S. T.; Murthy, N. N.; Weintraub, S. T.; Thompson, L. K.; Karlin, K. D. *Inorg. Chem.* **1997**, *36*, 956−957.
(27) (a) McKenzie, C. J.; Robson, R. *J. Chem. Soc., Chem. Commun.* **1988**, 112−114. (b) Hoskins, B. F.; McKenzie, C. J.; MacDonald, I. A. S.; Robson, R. *J. Chem. Soc., Dalton Trans.* **1996**, 2227−2232.
(28) Chen, G.; Edwards, T.; D'souza, V. M.; Holz, R. C. *Biochemistry* **1997**, *36*, 4278−4286.
(29) Addison, A. W.; Rao, T. N.; Reedijk, J.; van Rijin, J.; Verschoor, G. C. *J. Chem. Soc., Dalton Trans.* **1984**, 1349−1356.

Scheme 4. Preparative Route for [Co^{II}H$_2$P^{tBu}**uam**(OH)]$^{2-}$ [a]

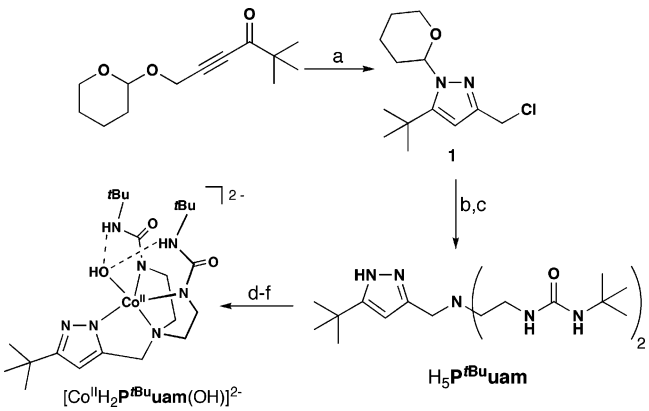

[a] Conditions: (a) $H_2NNH_2 \cdot H_2O$, MeOH, rt/HCl, MeOH, rt/$SOCl_2$, rt/1,2-dihyropyran, CH_2Cl_2, rt (57%); (b) $^{tBu}N_5$, Na_2CO_3, CH_3CN, Δ (85%); (c) ethanolic HCl/$NaCO_3$(aq) (98%); (d) 4 equiv of KH, DMA, rt, Ar; (e) 1 equiv of $Co(OAc)_2$, DMA, rt, Ar; (f) 1 equiv of H_2O, DMA, rt, Ar.

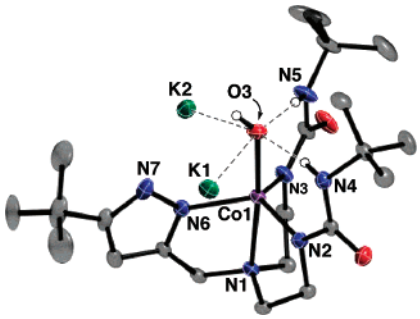

Figure 7. Molecular structure of [Co^{II}H$_2$P^{tBu}**uam**(OH)]$^{2-}$. The ellipsoids are drawn at the 50% probability level, and C-bonded H atoms are omitted for clarity.

Table 5. Selected Bond Distances (Å) and Angles (deg) for K$_2$[Co^{II}H$_2$P^{tBu}**uam**(OH)]·2DMA

Co1−N1	2.235(2)	N4···O3	2.774(3)
Co1−N2	2.0325(19)	N5···O3	2.783(3)
Co1−N3	2.0156(19)	K1···O3	2.826(2)
Co1−N6	2.044(2)	K2···O3	3.117(2)
Co1−O3	2.0441(18)		
N2−Co1−N3	121.16(8)	N6−Co1−N1	77.46(8)
N2−Co1−N6	117.07(7)	N2−Co1−O3	99.66(7)
N3−Co1−N6	112.84(7)	N3−Co1−O3	102.98(7)
N2−Co1−N1	81.41(7)	N6−Co1−O3	97.32(8)
N3−Co1−N1	80.87(7)	N1−Co1−O3	174.49(7)

The hydroxo ligand is terminal with a Co1−O3 bond length of 2.0441(18) Å, a distance significantly shorter than those found in [Co$^{II}_2$H$_4$P^{iPr}**buam**(μ-OH)]$^{2-}$ but comparable to that found in other monomeric five-coordinate Co^{II}−OH complexes possessing intramolecular H-bonds to the hydroxo O atom.[11] The N1−Co1−O3 angle is nearly linear at 174.49(7)°. Unlike in the molecular structure of the dimeric [Co$^{II}_2$H$_4$P^{iPr}**buam**(μ-OH)]$^{2-}$, there are two intramolecular H-bonds involving the hydroxo O atom O3 in [Co^{II}H$_2$P^{tBu}**uam**(OH)]$^{2-}$: this is indicated by N4···O3 and N5···O3 distances of 2.774(3) and 2.783(3) Å and the average N−H···O angle of 167(3)°. In addition, the cavity structure in [Co^{II}H$_2$P^{tBu}**uam**(OH)]$^{2-}$ is less constrained, leaving the Co^{II}−OH unit more exposed; in the crystal phase, this is evident by O3 interacting with the two K$^+$ counterions [K1···O3, 2.826(2) Å; K2···O3, 3.117(2) Å]. The crystal structure also shows that there are no intermolecular interactions between [Co^{II}H$_2$P^{tBu}**uam**(OH)]$^{2-}$ anions, suggesting that dimerization was prevented in the solid state.

Reactivity of [Co^{II}H$_2$P^{tBu}uam(OH)]$^{2-}$ with Acetonitrile and Ethyl Acetate. K$_2$[Co^{II}H$_2$P^{tBu}**uam**(OH)] was metathesized with 2 equiv of [^{n}Pr$_4$N]Cl to increase its solubility in acetonitrile; this was necessary to compare its reactivity to that of its dimeric [Co$^{II}_2$H$_4$P^{R}**buam**(μ-OH)]$^{2-}$. The spectroscopic properties of [^{n}Pr$_4$N]$_2$[Co^{II}H$_2$P^{tBu}**uam**(OH)] were the same as those of the potassium salt, including the same frequency for the O−H vibrations [ν(OH) = 3620 cm^{-1}].

[^{n}Pr$_4$N]$_2$[Co^{II}H$_2$P^{tBu}**uam**(OH)] does not hydrate acetonitrile; stirring the salt in acetonitrile for 2 h at room temperature under an argon atmosphere did not produce any spectroscopic changes in solution or in the isolated complex. Prolonged exposure to acetonitrile also does not produce evidence for hydration to an acetamide species. Similar observations were found when [^{n}Pr$_4$N]$_2$[Co^{II}H$_2$P^{tBu}**uam**(OH)] was treated with a 1:1 mixture of EtOAc and DMA. This salt was not able to hydrolyze ethyl acetate, and the isolated metal complex was determined as [Co^{II}H$_2$P^{tBu}**uam**(OH)]$^{2-}$. Taken together, these results suggest that a second metal ion in close proximity to the Co^{II}−OH unit is necessary for hydration/hydrolysis to occur.

In contrast, the potassium salt of [Co^{II}H$_2$P^{tBu}**uam**(OH)]$^{2-}$ does react with ethyl acetate; stirring K$_2$[Co^{II}H$_2$P^{tBu}**uam**(OH)] in a 1:1 mixture of DMA and ethyl acetate for 2 h at room temperature under an argon atmosphere produced changes in the spectroscopy of the isolated complex. The most obvious differences were the absence of the peak associated with the O−H vibration and the appearance of a strong ν(NH) signal at 3361 cm^{-1}, suggesting a change in the H-bonding network. In addition, a white solid precipitated from the pink-purple reaction mixture, which was identified by FTIR spectroscopy as KOAc. Moreover, attempts to recrystallize K$_2$[Co^{II}H$_2$P^{tBu}**uam**(OH)] in a 1:1 DMA/ethyl acetate solution using vapor diffusion of diethyl ether produced a white solid product, which analyzed as KOAc in nearly quantitative yield.

This difference in reactivity between the two salts of [Co^{II}H$_2$P^{tBu}**uam**(OH)]$^{2-}$ can be accounted for by assuming that the K$^+$ ion(s) function(s) as the additional metal ion during hydrolysis. The solid-state structure of K$_2$[Co^{II}H$_2$P^{tBu}**uam**(OH)] indicates that the H-bond cavity surrounding the Co^{II}−OH unit is large enough to allow K$^+$ ions to interact with the hydroxo ligand. Similar interactions could occur in solution, which would help facilitate the hydrolysis of ethyl acetate. When no additional metal ions are present, as in the tetrapropylammonium salt, reactivity is not possible because the [H$_2$P^{tBu}**uam**]$^{3-}$ ligand prevents intermolecular interactions between two Co^{II} complexes. Although K$_2$[Co^{II}H$_2$P^{tBu}**uam**(OH)] hydrolyzes esters, it does not react with acetonitrile: no IR or optical changes were observed when the salt was dissolved in a 1:1 mixture of DMA/acetonitrile and stirred for at least 2 h. Contributing factors to this lack of reactivity is that K$^+$ ions have a higher affinity for O atoms over N atoms and carboxy esters are more labile toward hydrolysis than nitriles.

Summary and Conclusions

This work described synthetic methods for preparing dimeric $Co^{II}-\mu$-X′$-Co^{II}$ complexes using the pyrazolate-based ligands H_9**P^{R}buam**, where X′ = OH^-, $[OC(NH)CH_3]^-$, and OAc^-. The $Co^{II}-\mu$-OH$-Co^{II}$ complex was obtained through the addition of water and the presence of an intramolecular base positioned within the cavity through deprotonation of one of the α′NH groups.[11] The dual function of the synthetic cavity in these complexes resembles active sites found in metalloproteins by utilizing H-bonds and general basic sites to control functional properties.

$[Co^{II}_2H_4$**P^{R}buam**$(\mu$-OH$)]^{2-}$ was found to react stoichiometrically with unactivated nitriles and esters under ambient conditions: this was illustrated with the hydration of acetonitrile and the hydrolysis of ethyl acetate at room temperature to afford $[Co^{II}_2H_4$**P^{R}buam**$(\mu$-1,3-OC(NH)-$CH_3)]^{2-}$ and $[Co^{II}_2H_4$**P^{R}buam**$(\mu$-1,3-OAc$)]^{2-}$. X-ray diffraction studies on the $Co^{II}-\mu$-1,3-X′$-Co^{II}$ products (X′ = $[OC(NH)CH_3]^-$ and $^-$OAc) reveal that the superstructures of the cavities provide four H-bond donors that are directed intramolecularly toward the bridging ligands. This results in the formation of intramolecular H-bonds with the hydrated/hydrolyzed products bound within the cavity, illustrating some control within the secondary coordination sphere. Additional control of the secondary sphere is provided by the alkyl groups appended from the urea arms, as seen in the molecular structures of $[Co^{II}_2H_4$**P^{R}buam**$(\mu$-1,3-OAc$)]$. The large differences in fold angles of the bound acetate bridge demonstrate how the alkyl groups affect the size of the H-bonding pocket.

The proposed mechanism of hydration/hydrolysis suggests that the H-bonding network within the synthetic "active site" may function to orient the substrate, stabilizing a reactive terminal hydroxo intermediate and stabilizing the hydrated/hydrolyzed product. Similar shifts in the binding mode of the hydroxo ligand have been suggested in studies done on binuclear metallohydrolases such as aminopepidases.[28] The mononuclear $Co^{II}-$OH complex $[Co^{II}H_2$**P^{tBu}uam**$(OH)]^{2-}$ was also prepared, and its reactivity is consistent with the need for two metal ions to accomplish the hydration/hydrolysis reactions. Hydrolysis of ethyl acetate to acetate was only observed with $K_2[Co^{II}H_2$**P^{tBu}uam**$(OH)]$, suggesting that the K^+ counterions may act as the second metal ion to assist in activating the substrate. The open-cavity structure in $[Co^{II}H_2$**P^{tBu}uam**$(OH)]^{2-}$ supports the view that K^+ ions can interact with the $Co^{II}-$OH unit.

Acknowledgment. We thank the NIH (Grant GM50781) for financial support and the NSF (Grant CHE-0079282) for funding of the X-ray diffraction instrumentation.

Supporting Information Available: Spectral data (Figures S1−S3) for $[Co^{II}_2H_4$**P^{R}buam**$(\mu$-X$)]^{2-}$ (R = ^{t}Bu, ^{i}Pr and X = OH^-, $[OC(NH)CH_3]^-$, and OAc^-) and completed details for the X-ray diffraction experiments, including CIFs, with thermal ellipsoid plots of $[Co^{II}_2H_4$**P^{iPr}buam**$(\mu$-OH$)_{0.82}(\mu$-Cl$)_{0.18}]^{2-}$, $[Co^{II}_2H_4$**P^{iPr}buam**$(\mu$-1,3-OC(NH)$CH_3)_{0.90}$(Cl$)_{0.10}]^{2-}$, and $[Co^{II}_2H_4$**P^{tBu}buam**$(\mu$-1,3-OC-(NH)$CH_3)]^{2-}$ (Figures S4−S6). This material is available free of charge via the Internet at http://pubs.acs.org.

IC700685G